Granular Mechanics of Geomaterials

(presentation in Cassino, Italy, 2006)

Takashi Matsushima University of Tsukuba

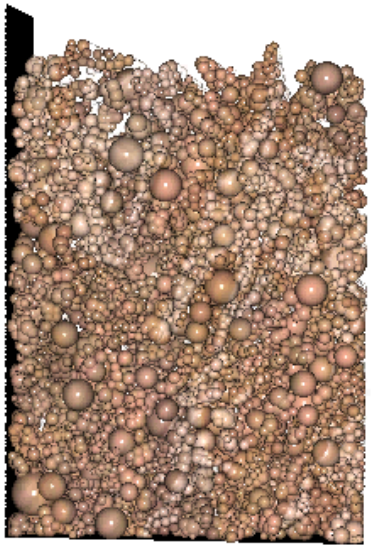

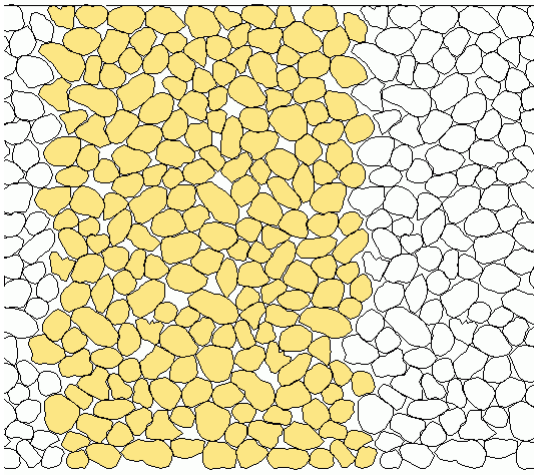

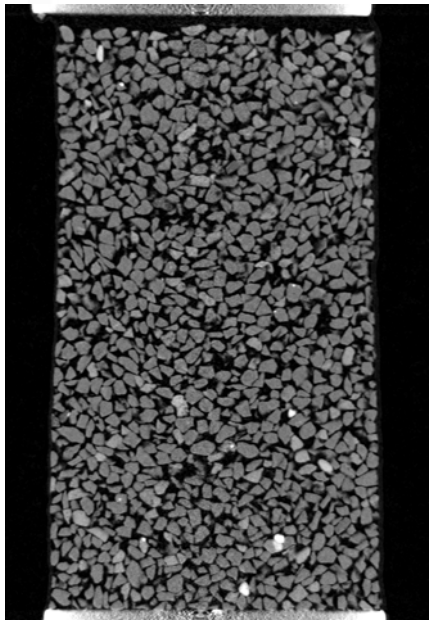

Where am I from?

What is granular mechanics?

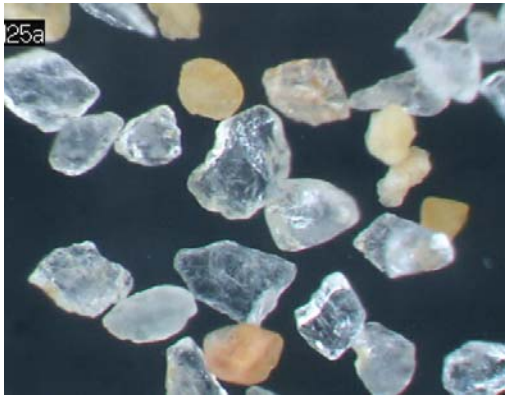

Particle characteristics
(size, shape, crushability etc.)

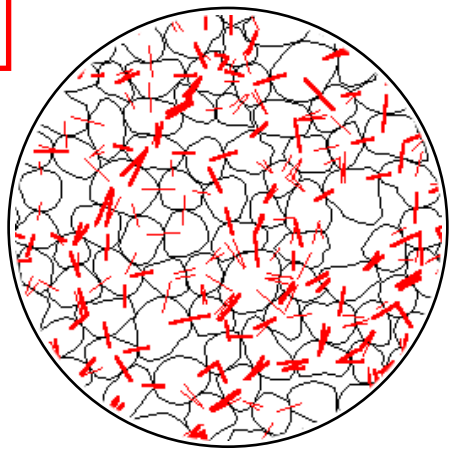

Particle interaction

Direct simulation
(by DEM etc.)

Constitutive model as solid or fluid

Simulation as continua
(by FEM, SPH etc.)

No element test!?

Lunar exploration

Mechanical properties of Lunar soil is needed.

But only TWO TC test results is available.

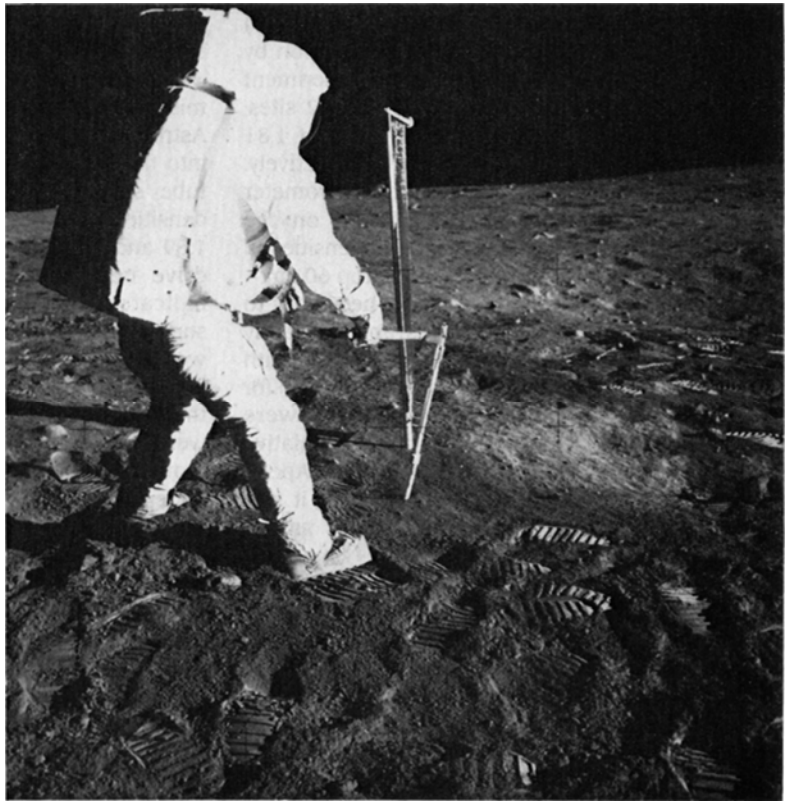

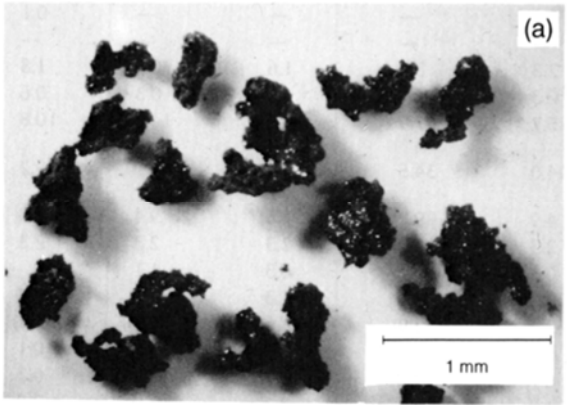

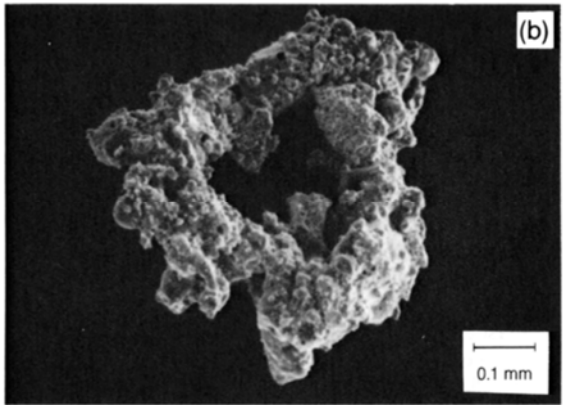

Lunar regolith:
very angular
well graded sand

Lunar sourcebook, 1991

Why granular mechanics?

***TRUE prediction**

from particle information

eg.

Mechanics of crushable soil

Mechanics of unsaturated soil

Mechanics of cemented soil

and more…

***UNIQUE constitutive model**

more convincing, more rational

Contents:

1. Theory of granular mechanics

Chang and Misra 1990, Matsushima and Chang 2006

2. Micro X-ray CT experiment

Matsushima et al. 2002-

3. Image-based DEM simulation

Matsushima 2002-

incl. recent application to Lunar exploration

Matsushima 2006

Basic theories

Molecular dynamics

Statistical mechanics for molecules

(sparse, non-frictional)

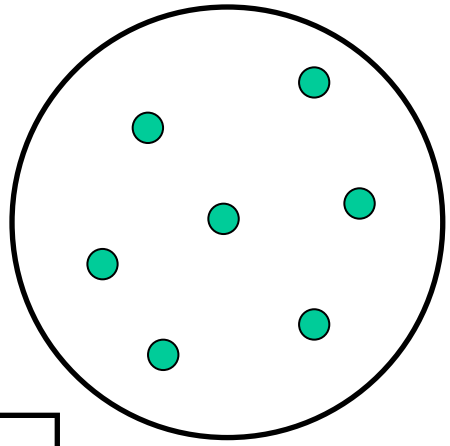

Mechanics of solid frictional particles

Kinetic theory

(sparse→behaves as a fluid)

+

Mechanics of geomaterials

(dense →behaves as a solid)

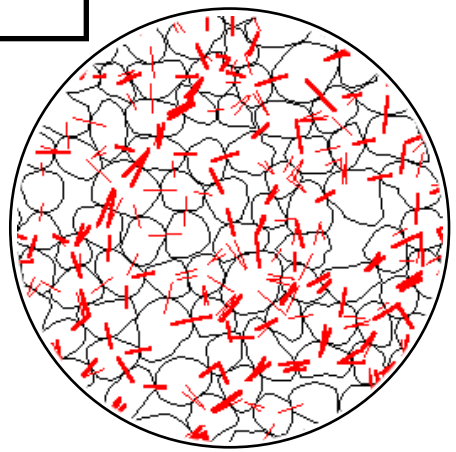

Uniform strain model (Chang and Misra 1990)

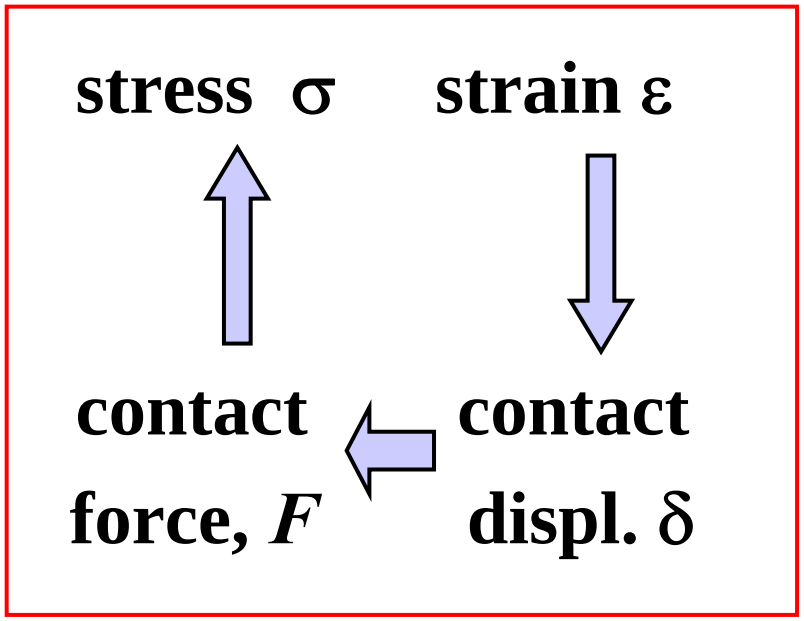

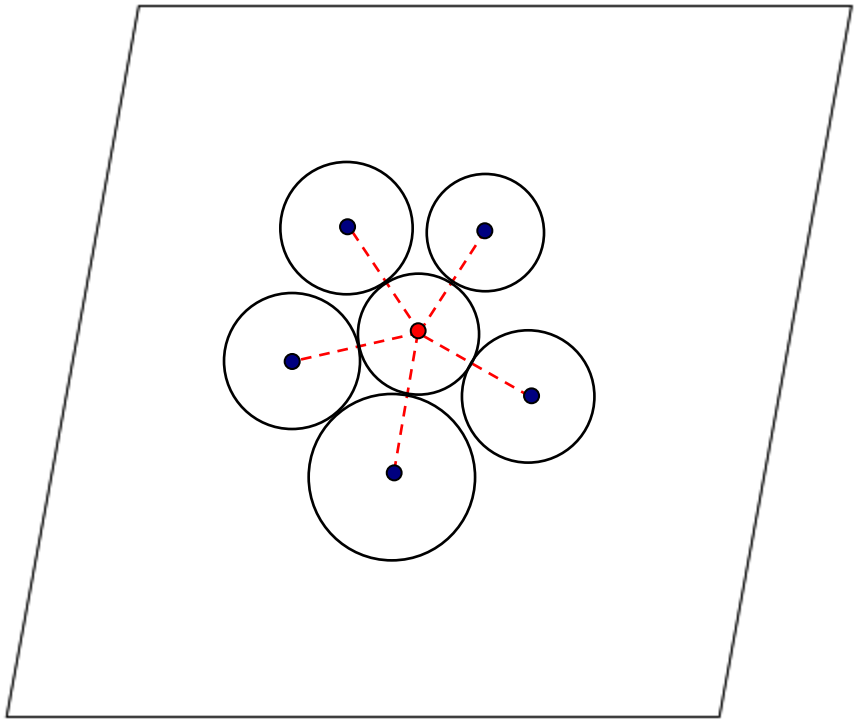

*Grain controids stick to continuum deformation field

*Grain rotation coincides with continuum rotation

→ contact displ. δ

Contact displ.→Contact force→Stress

Global →local coordinates

$$\boldsymbol{\delta}^L = \boldsymbol{R}^T \cdot \boldsymbol{\delta}$$

Force-displ. relation at contact

$$\boldsymbol{f}^L = \begin{pmatrix} f_n \\ f_s \end{pmatrix} = \begin{pmatrix} k_n & 0 \\ 0 & k_s \end{pmatrix} \cdot \boldsymbol{\delta}^L$$

Global local coordinates

$$\boldsymbol{f} = \boldsymbol{R} \cdot \boldsymbol{f}^L$$

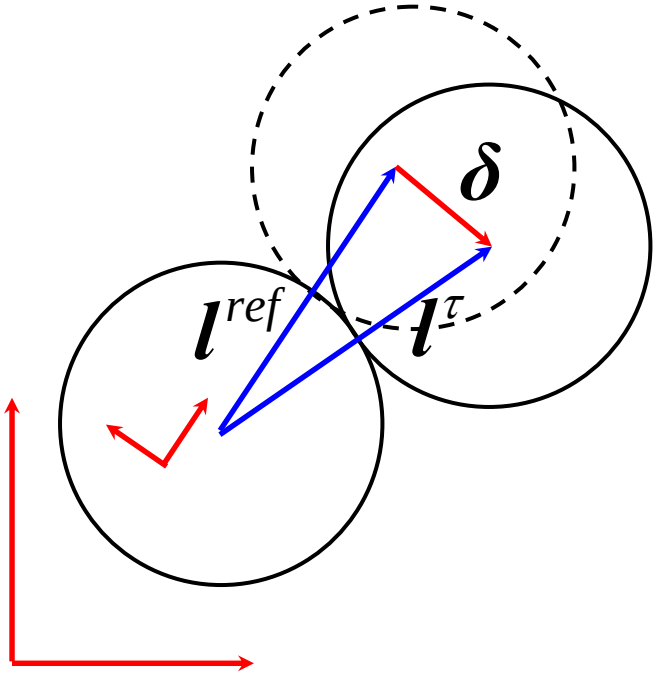

Stress

$$\boldsymbol{\sigma}^{t^T} = \frac{1}{V_R^t} \sum_c (\boldsymbol{l}^t \otimes \boldsymbol{f}^t)$$

Sum of contacts in V_R

work at contact = work as continuum

Elastic solution

Assuming

equal-sized isotropic sphere packing…

$$\overline{E} = \frac{2r^2 N}{15V}(2k_n + 3k_s)\left(\frac{5k_n}{4k_n + k_s}\right)$$

$$\overline{\nu} = \frac{k_n - k_s}{4k_n + k_s}$$

$$\frac{N}{V} = \frac{3n}{4\pi r^3(1+e)}$$

e-*n* relation is necessary

n : coordination number

Overall Young's modulus and Poisson ratio can be described by contact stiffness

Elastic solution (continued..)

Applying Hertz-Mindlin contact law… (Johnson,Contact mechanics)

$$\dot{f}_n = \left(\frac{\sqrt{3r}\,G}{1-\nu}\right)^{2/3} f_n^{\,1/3}\,\dot{\delta}_n \equiv k_n\,\dot{\delta}_n \qquad \dot{f}_s = \frac{2(1-\nu)}{2-\nu} k_n \left(1-\frac{f_s}{f_n \tan\phi_\mu}\right)^{1/3} \dot{\delta}_s \equiv k_s\,\dot{\delta}_s$$

$$\overline{E} = \frac{2r^2(5-4\nu)}{3(5-3\nu)}(9\sigma_0)^{1/3}\left[\frac{GN}{(1-\nu)V}\right]^{2/3}$$

$$\overline{\nu} = \frac{\nu}{2(5-3\nu)}$$

$$\overline{G} = \frac{\overline{E}}{2(1+\overline{\nu})} = A\cdot\left(\frac{n(e)}{1+e}\right)^{2/3}(\sigma_0)^{1/3}$$

$$n(e) = 2.63 - 1.79e$$

$$A = \frac{2r^2(5-4\nu)}{15(2-\nu)}(9)^{1/3}\left[\frac{3G}{4\pi r^3(1-\nu)}\right]^{2/3}$$

$\overline{G}$ is a function of confining pressure, σ_0 and void ratio, e

Smith et al. (1929) by the combination of closest and loosest packing

Elastic solution (continued..)

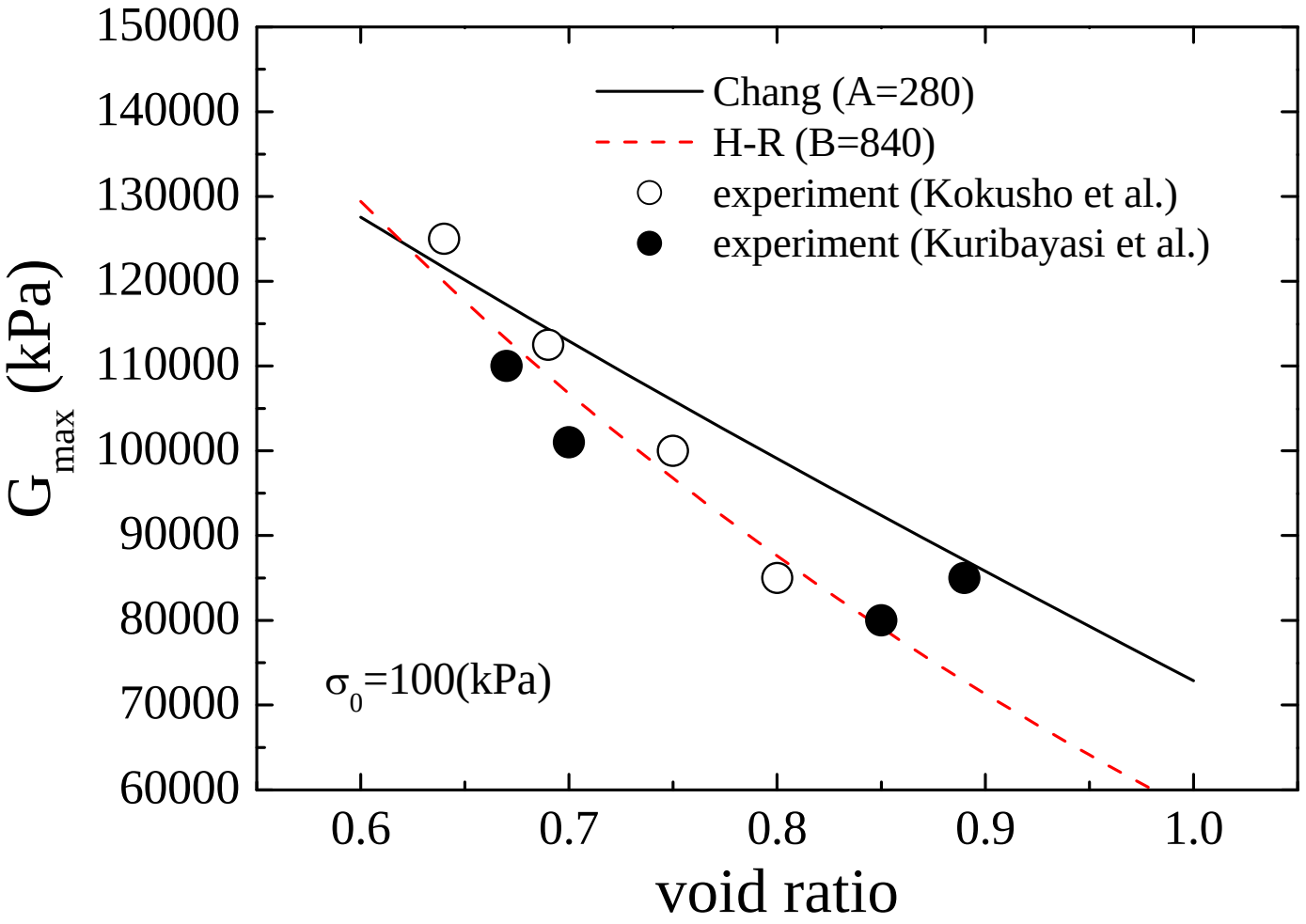

Cf. Hardin & Richart $\overline{G} = B \cdot \dfrac{(2.17-e)^2}{1+e} (\sigma_0)^{1/2}$

Elastic solution (continued..)

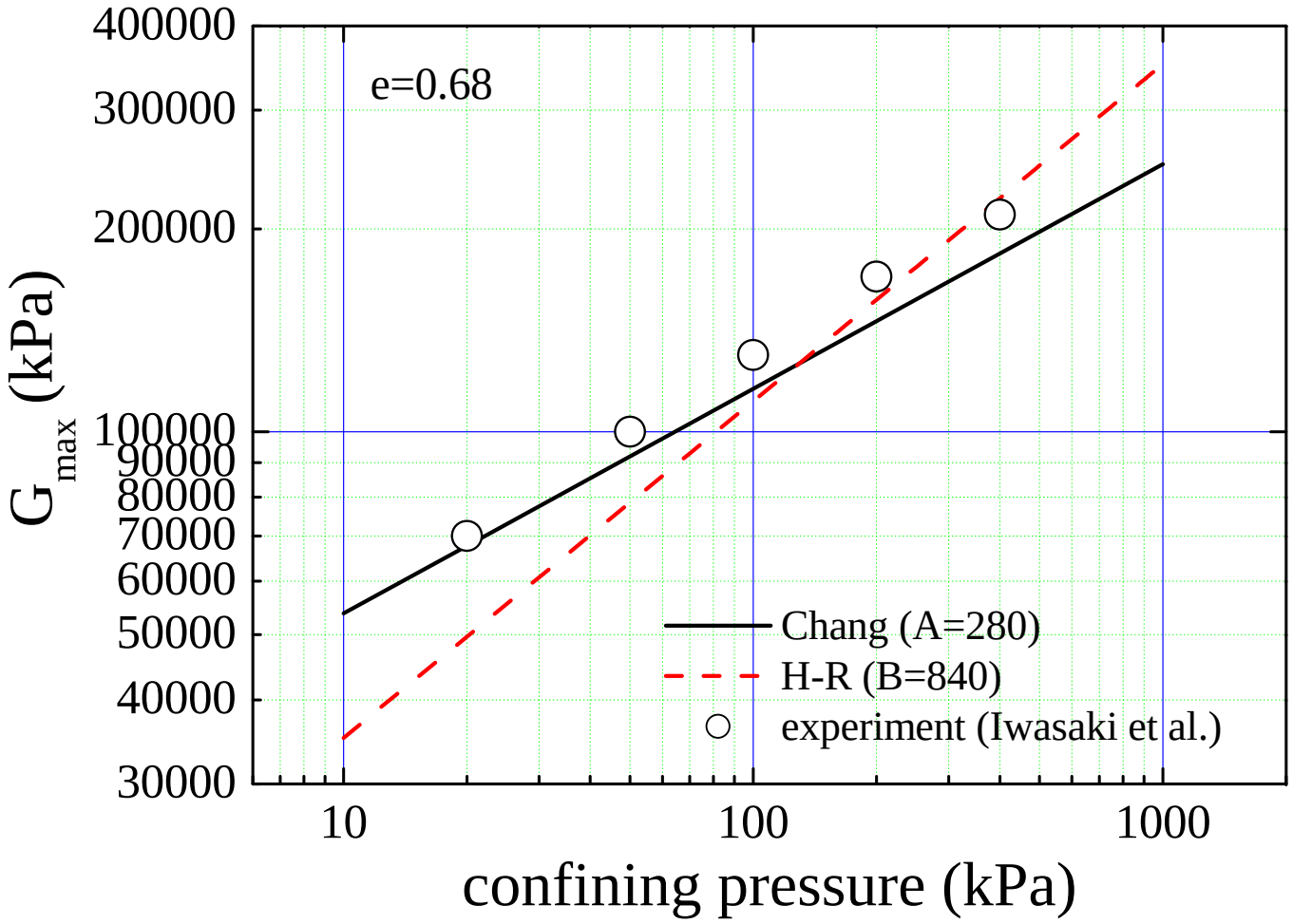

Cf. Hardin & Richart $\overline{G} = B \cdot \frac{(2.17-e)^2}{1+e} (\sigma_0)^{1/2}$

Elastic solution (continued..)

Note:

A=280 corresponds to

G=73(GPa), ν=0.25 (sand particle as a solid)

Estimation of $\overline{\nu}$ is not good.

(Further research is necessary.)

Nonlinear model

- Loss of contact
  is considered by tension-free model

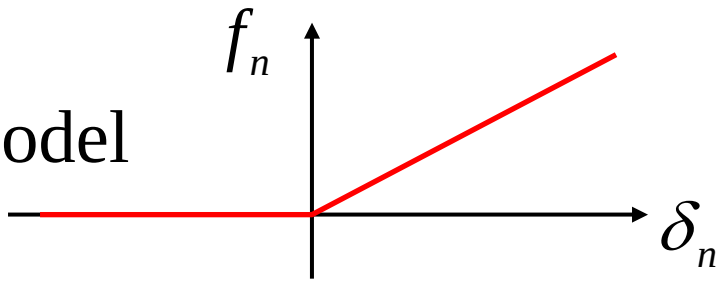

- Contact slip (plasticity)

$$|f_s| \begin{cases} \leq -\mu f_n & \rightarrow (elastic) \\ > -\mu f_n & \rightarrow (sliding) \rightarrow |f_s| = -\mu f_n sign(f_s) \end{cases}$$

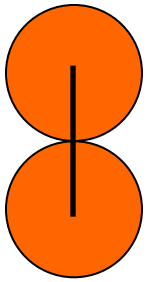

Analytical solution is not available.
→A set of branch vectors are assumed
and the solution is obtained numerically.

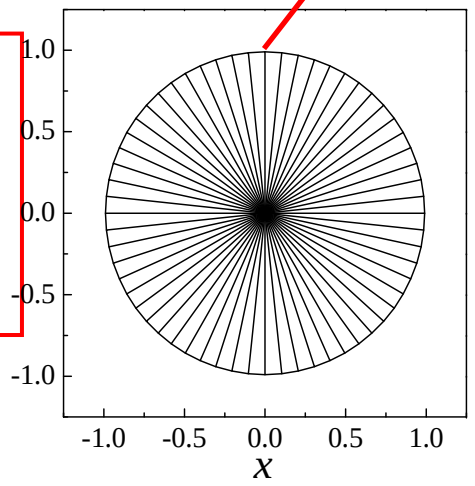

Basic response (biaxial compression)

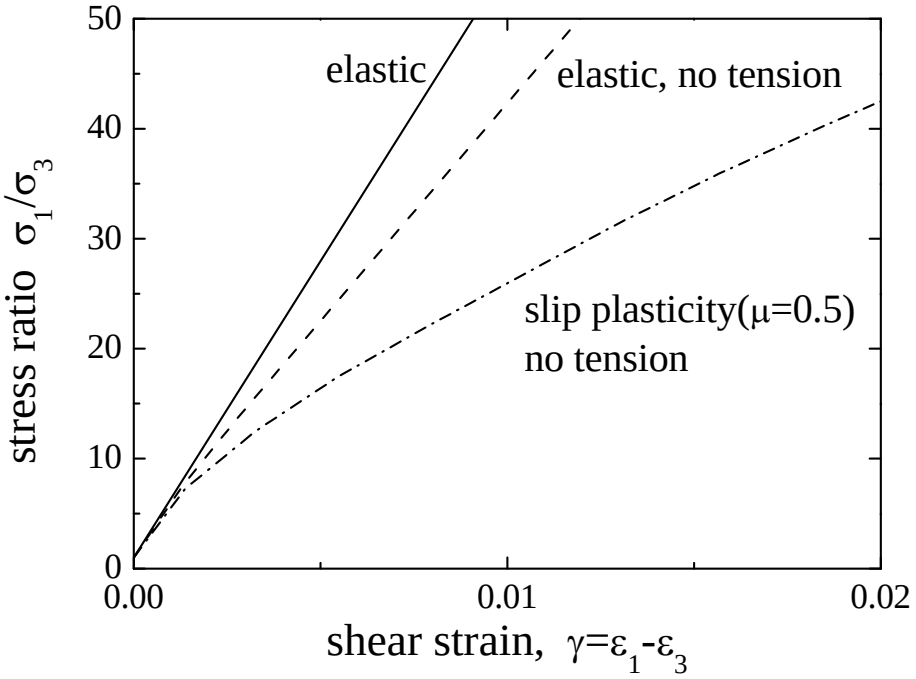

stress-strain curve

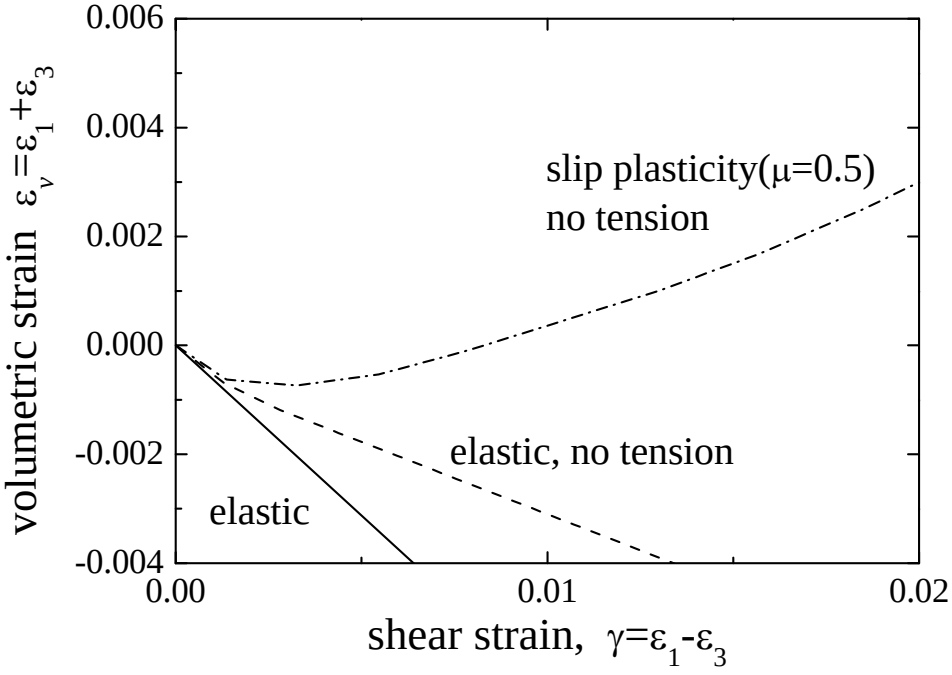

dilation curve

Material does NOT yield!

Basic response (biaxial compression)

Why?

Contact of loading direction does NOT slip.

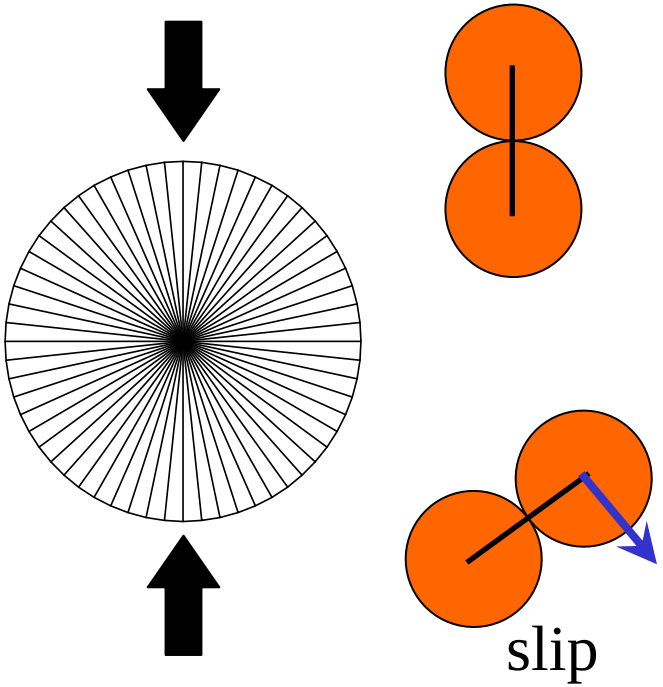

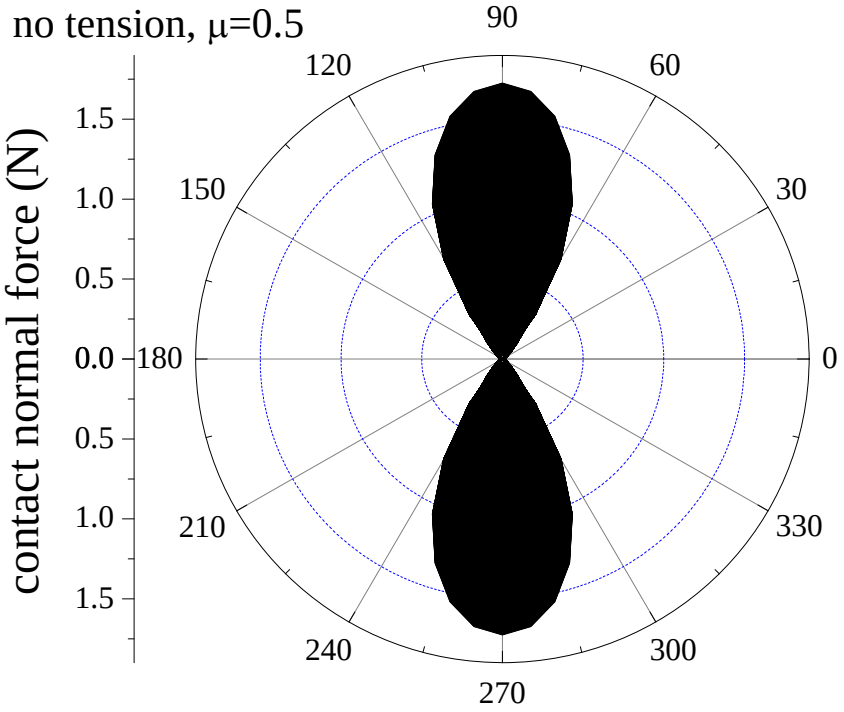

Contact normal force distribution

DEM study

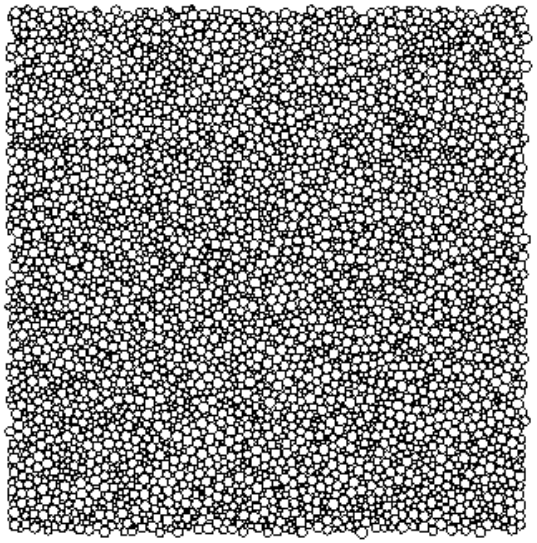

periodic boundaries
at both directions

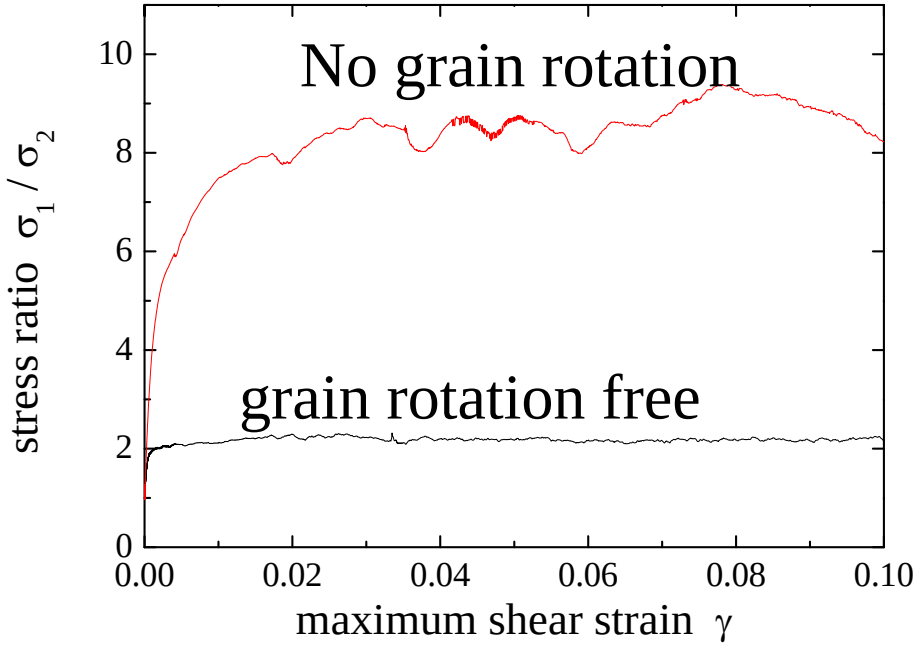

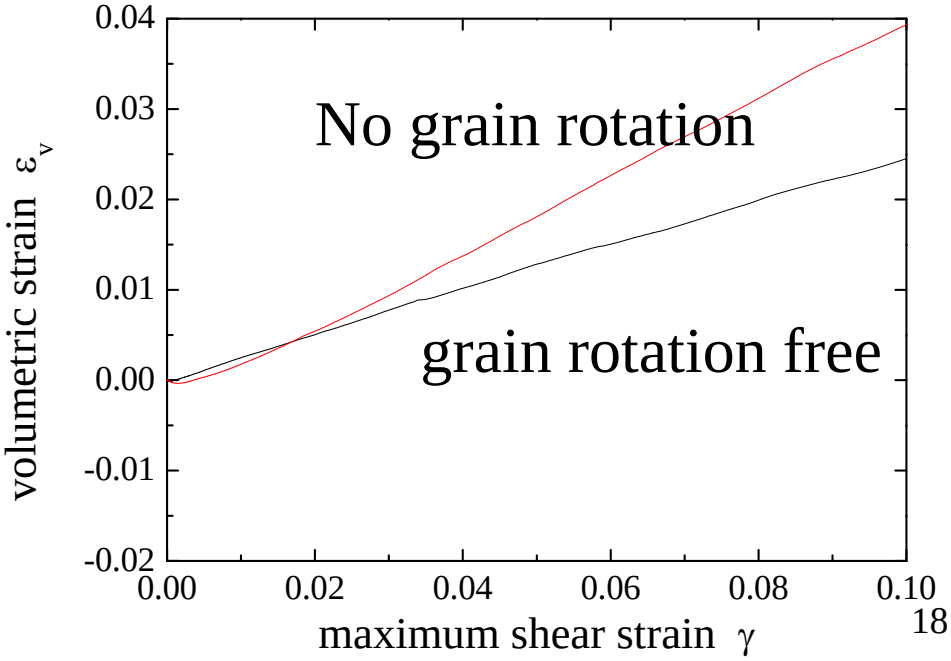

DEM study

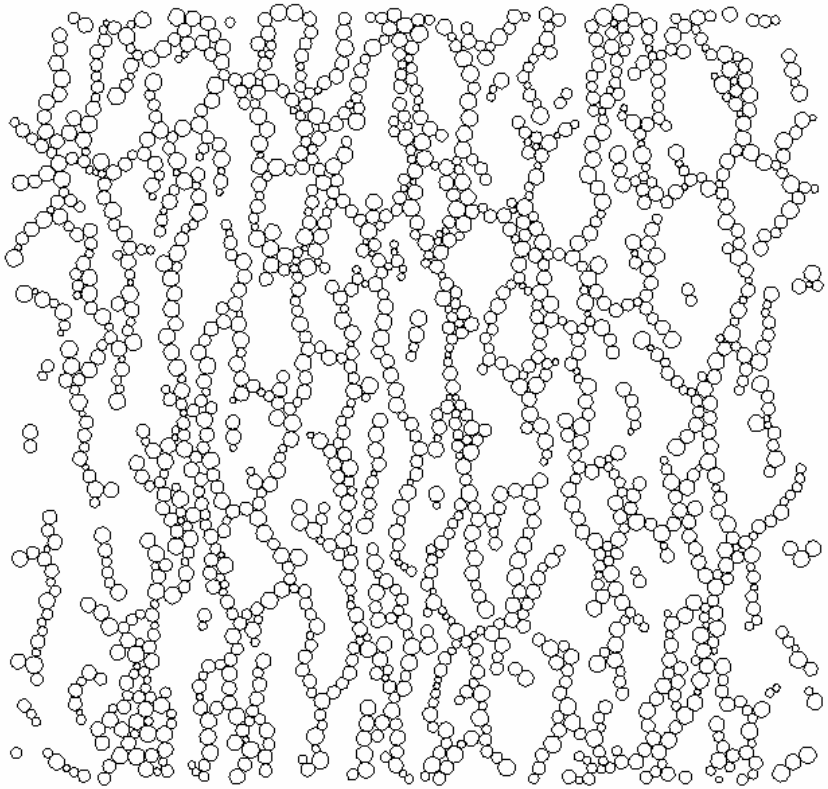

Force chain
in granular assembly

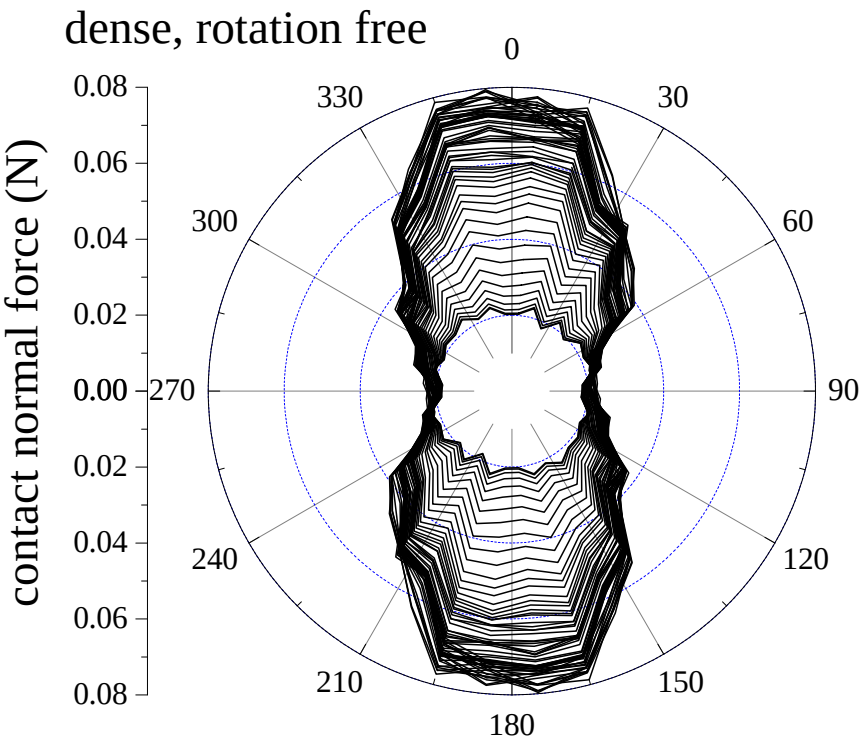

Contact normal force
distribution

Buckling of granular column

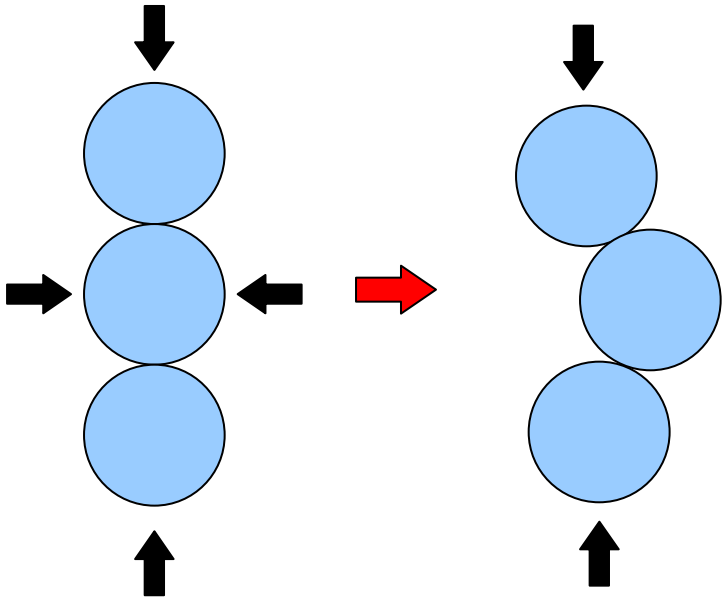

(Matsushima and Chang, 2006)

- Assign minimum aspect ratio for contact force distribution
- Determine average contact force such that the stored energy in contact keeps constant

insufficient confining pressure

↓

buckling

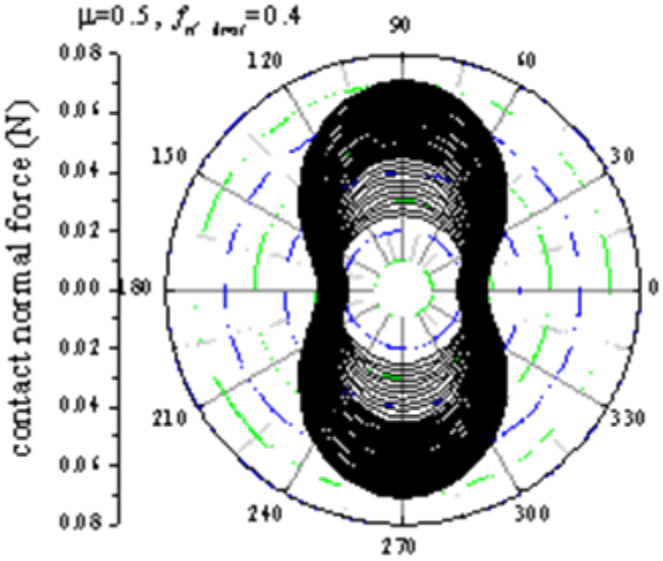

Response of Buckling model

(Matsushima and Chang, 2006)

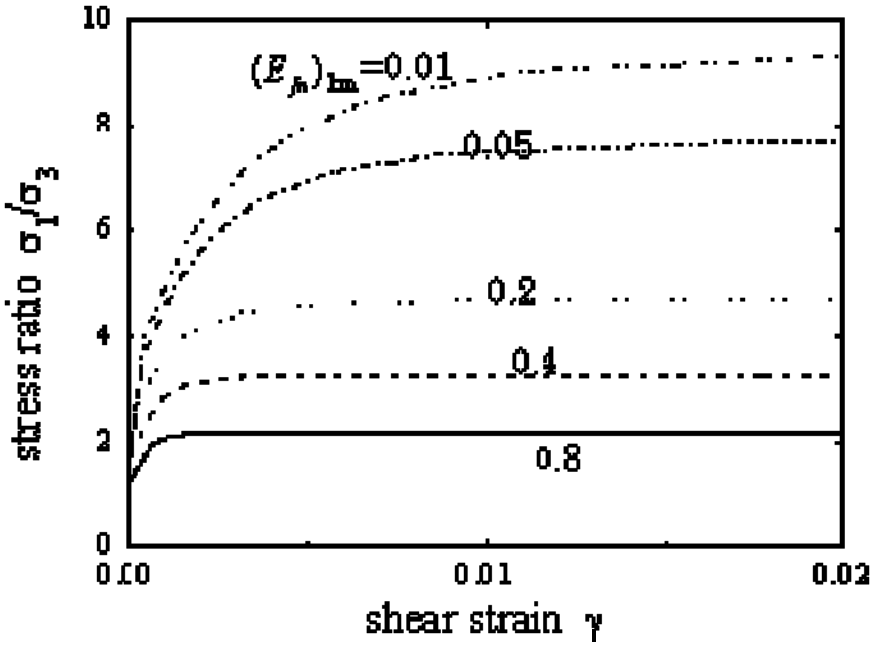

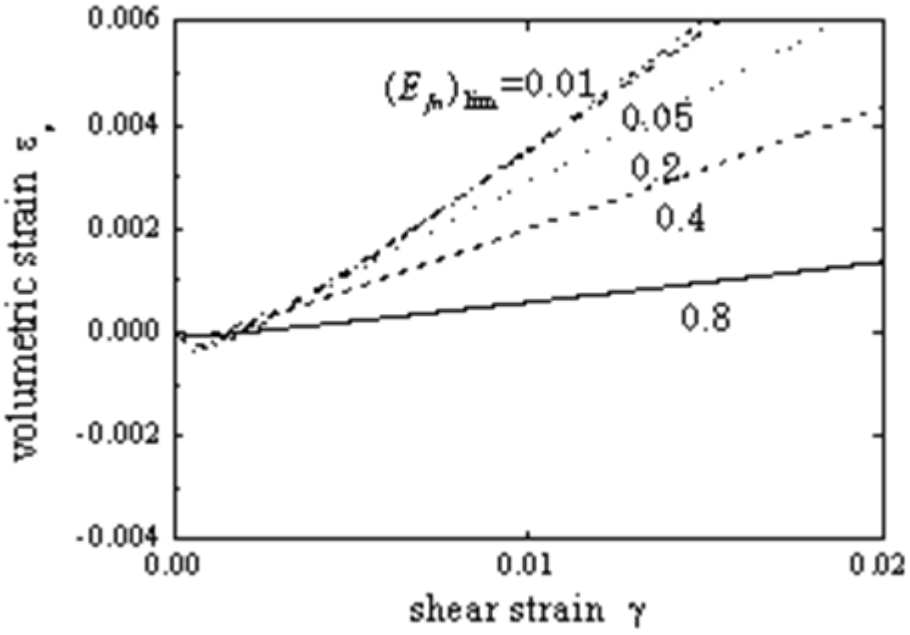

Buckling resistance controls the yield strength

related to particle properties

Possibility of granular mechanics C.E.

Rational incorporation of particle properties
(size, shape, stiffness, crushability, contact cement, etc.)

Validation not only with macro response
but also with particle-level information

Detailed comparison with

Particle visualization experiment

More realistic DEM

is needed.

Particle visualization by Micro X-ray CT

At University Joseph Fourier, Grenoble, 2002

Objective

to obtain 3-D micro properties
(grain properties, microstructure
and its change due to external loading)
of some standard sands
with micro X-ray CT in SPring-8

Typical standard sands:

Toyoura sand: D_{50} =0.167(mm)
Ottawa sand: D_{50} =0.174(mm)
Hostun sand: D_{50} =0.408(mm)
S.L.B. sand: D_{50} =0.681(mm)

(high resolution system is necessary)

Micro X-ray CT at Spring-8

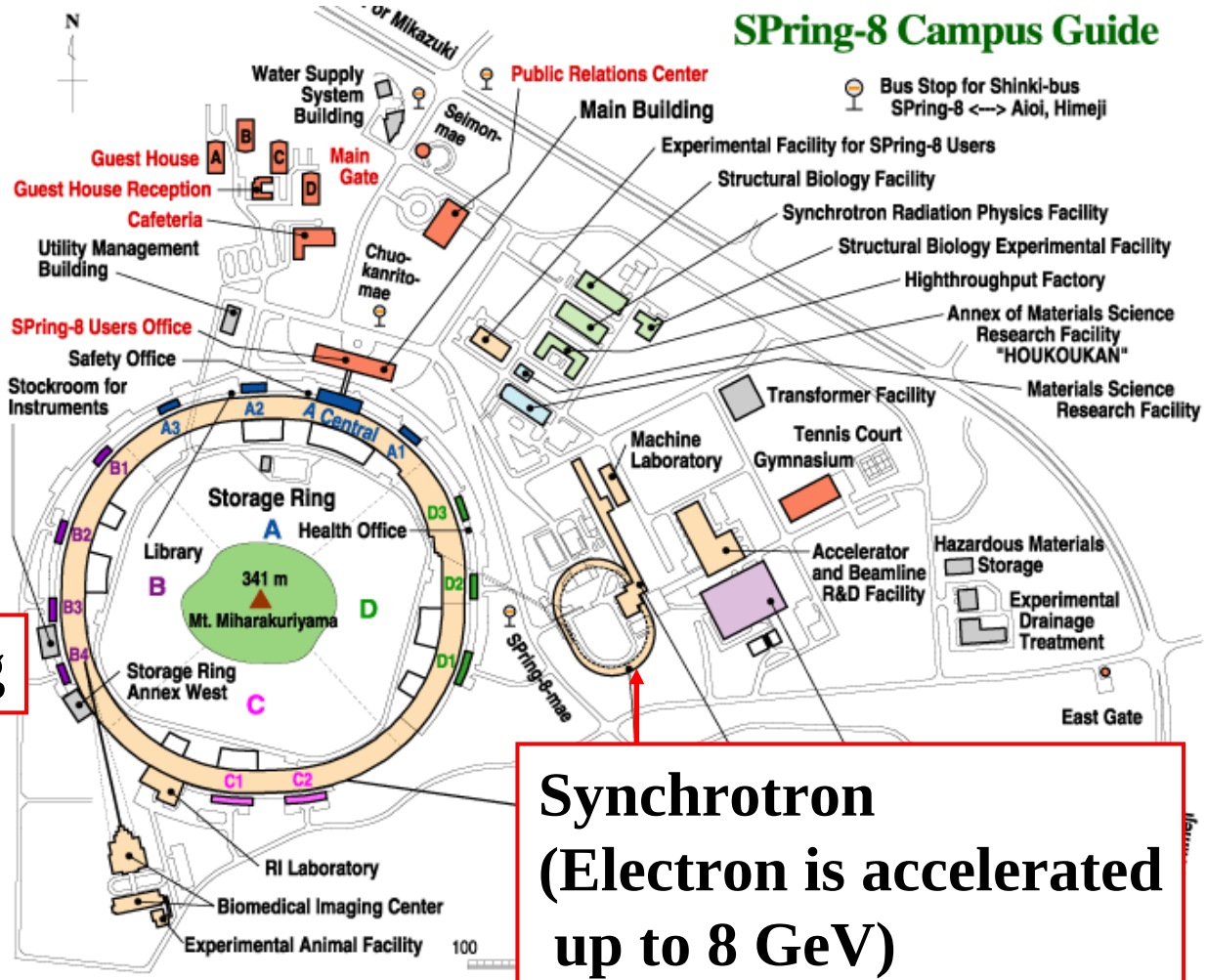

Storage Ring

Synchrotron (Electron is accelerated up to 8 GeV)

The world's largest third-generation synchrotron radiation facility

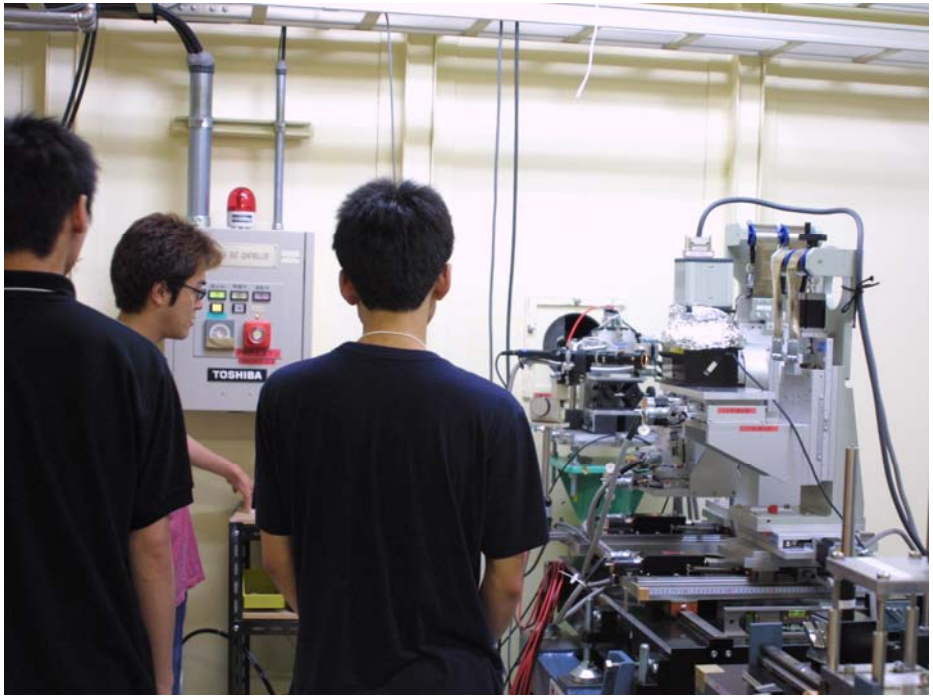

47 beamlines (BL)

X-ray CT is available at BL20B2 and BL47XU.

Outline of Spring-8

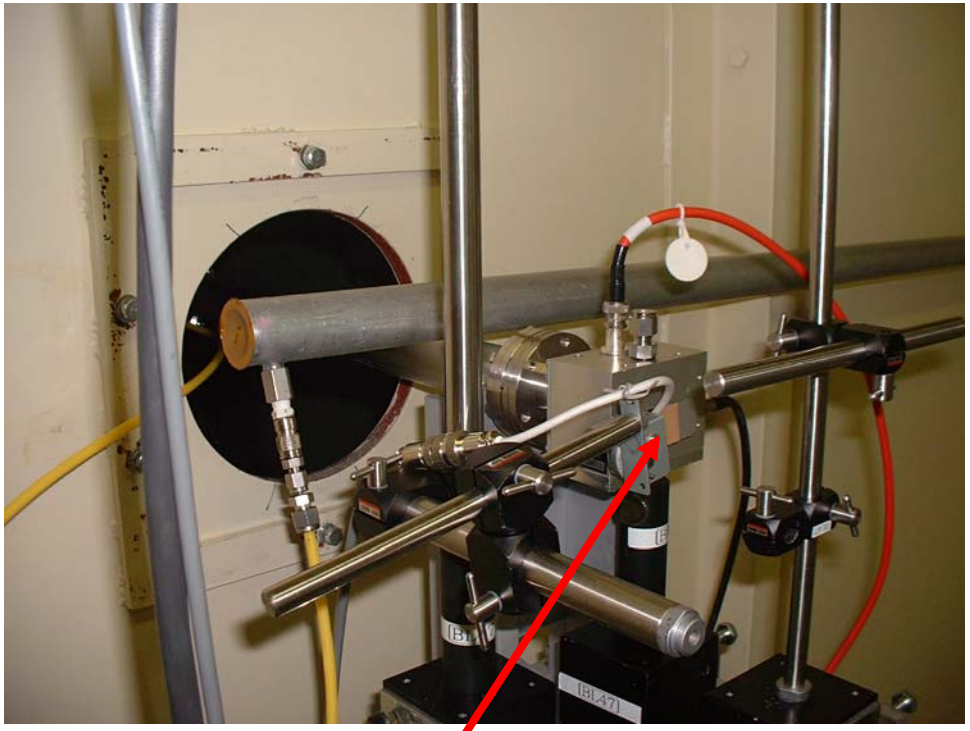

X-ray comes from here

CCD camera

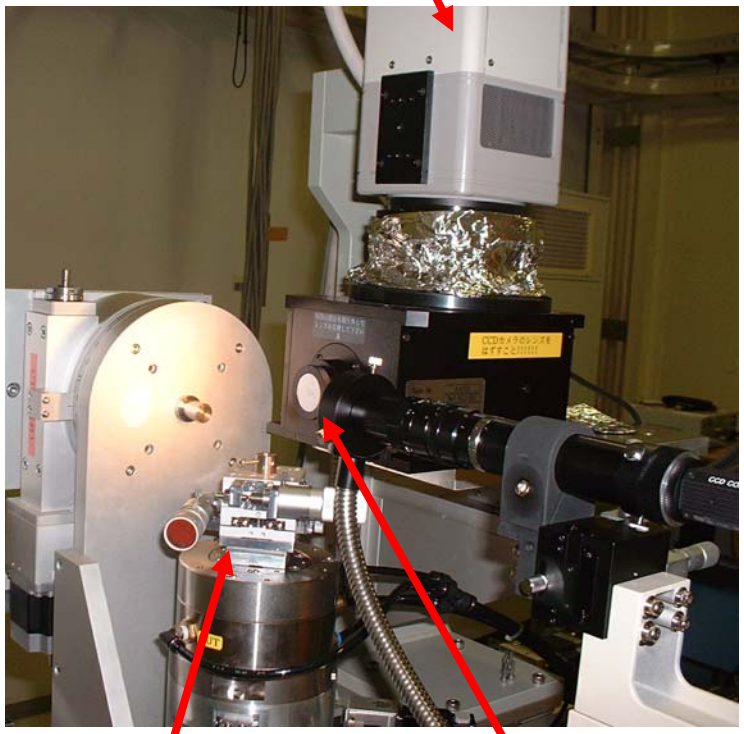

Stage

Detector

X-ray CT system at SPring-8

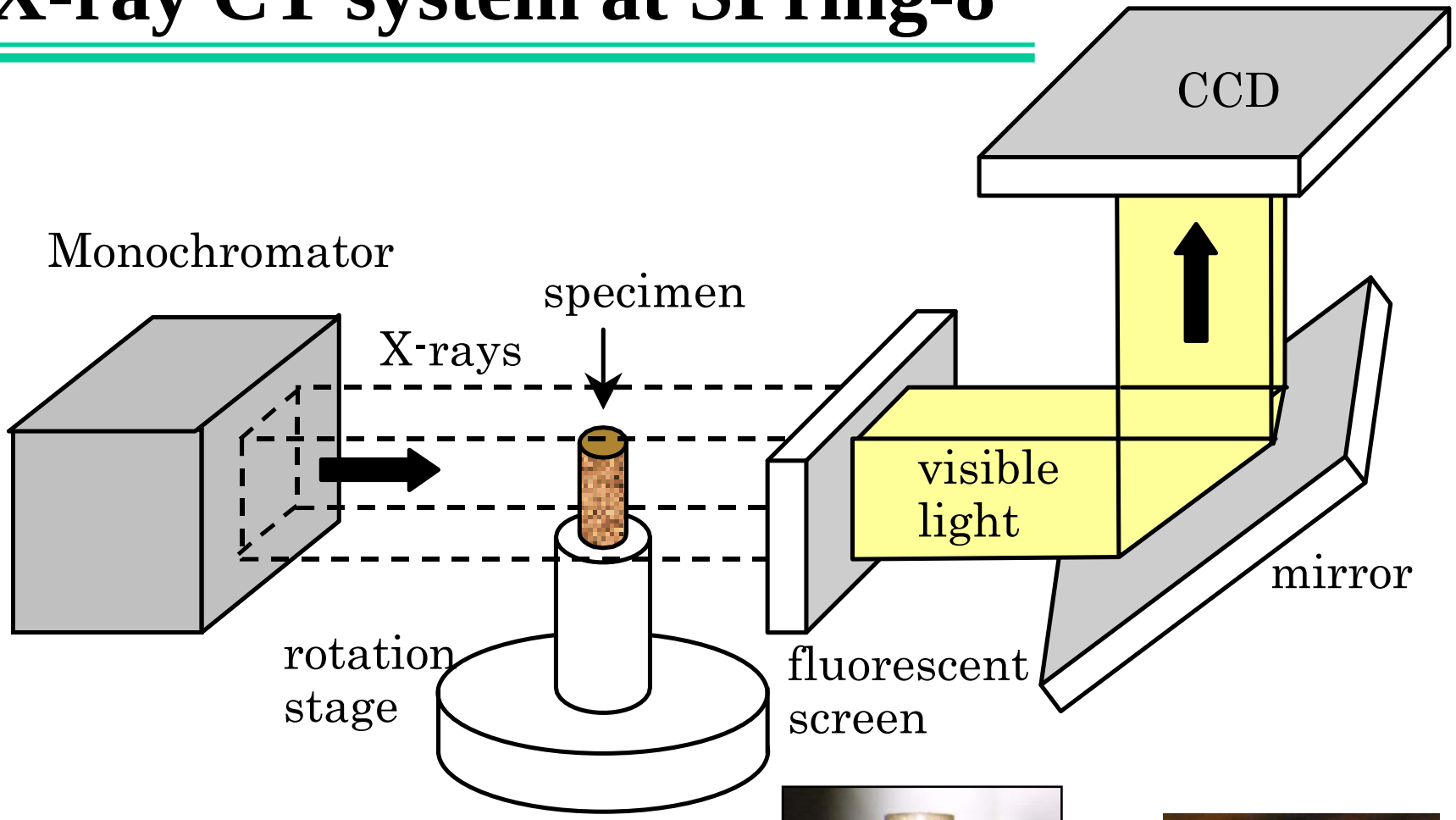

Resolution:
BL20B2: 13 μm
BL47XU: 1.5 μm

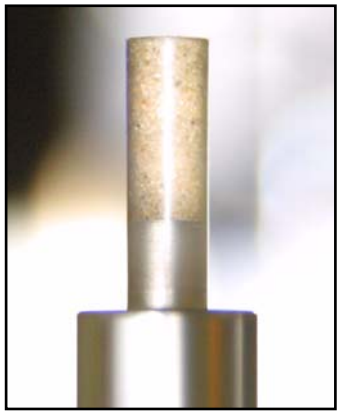

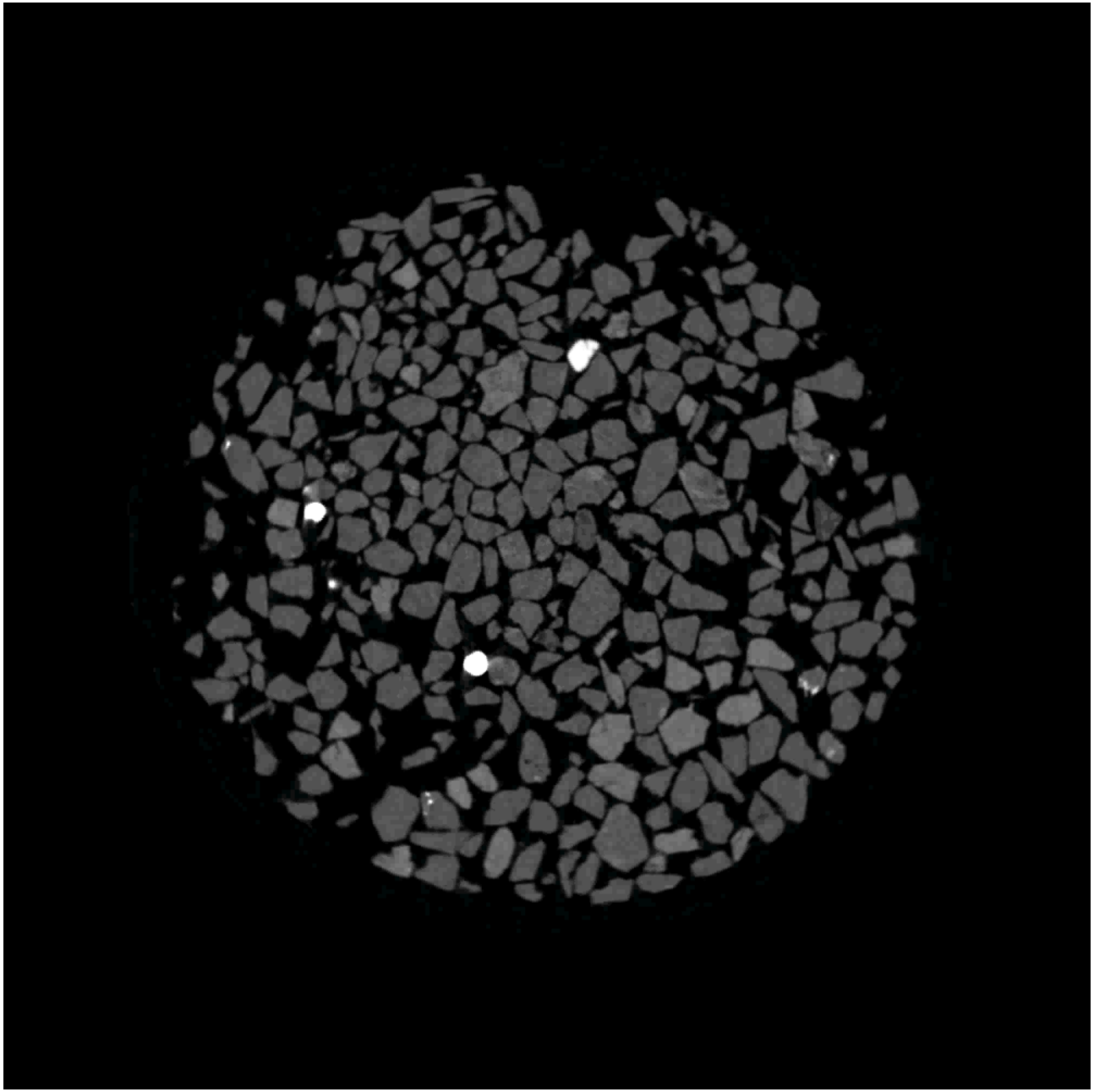

Toyoura sand dense

Example of CT image (BL20B2)

Toyoura sand

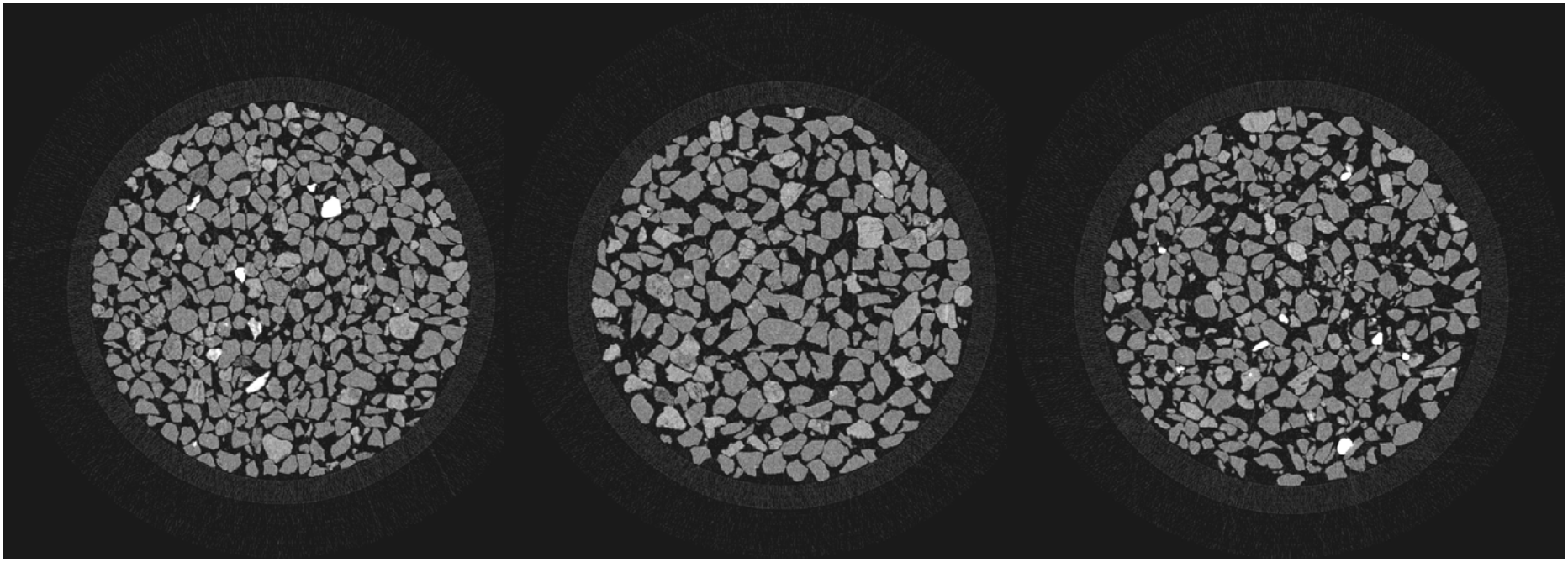

dense　　medium dense　　loose

Example of CT image (BL20B2)

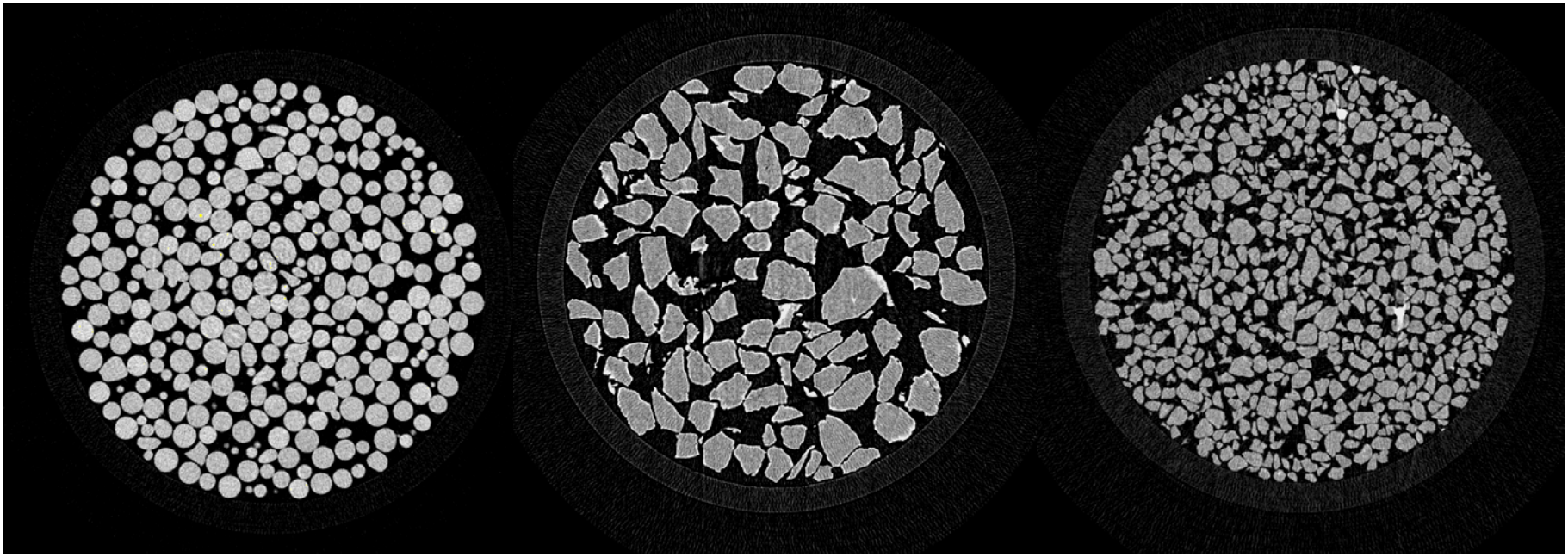

Glass beads **Hostun sand** **Ottawa sand**

Example of CT image (BL47XU)

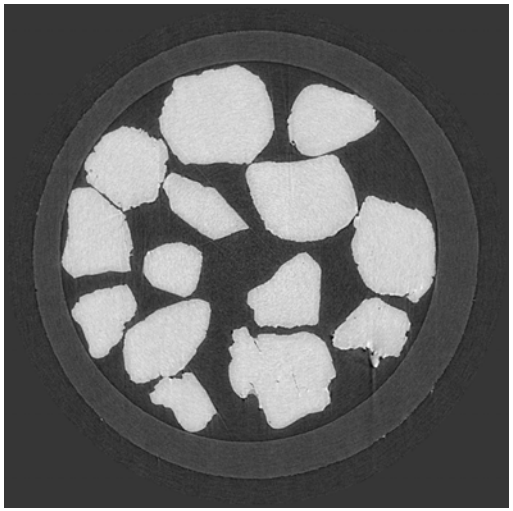

Ottawa sand

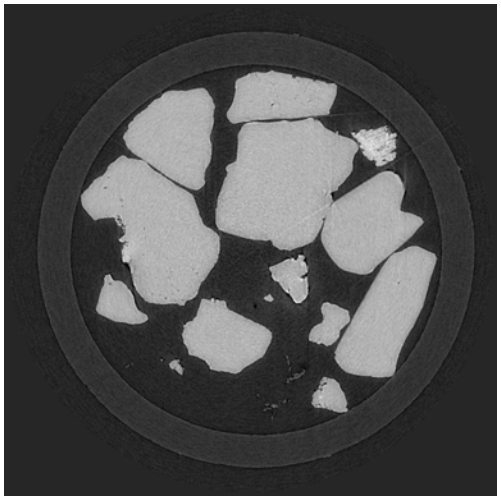

Toyoura sand

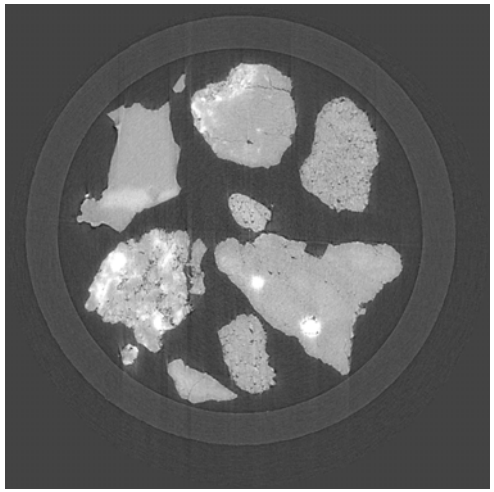

Wakasa sand

Roundish

very angular

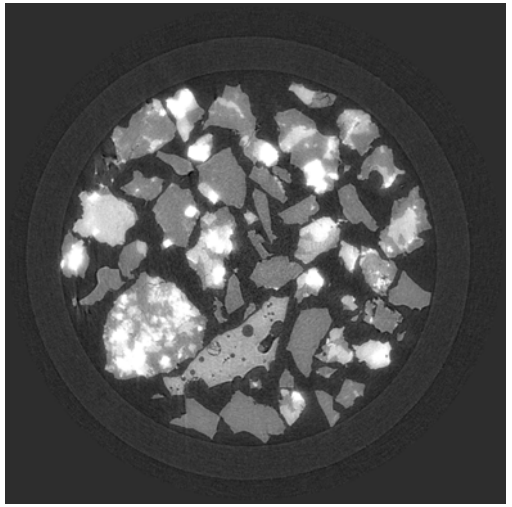

Lunar soil simulant(FJS-1)

Example of CT image (BL47XU)

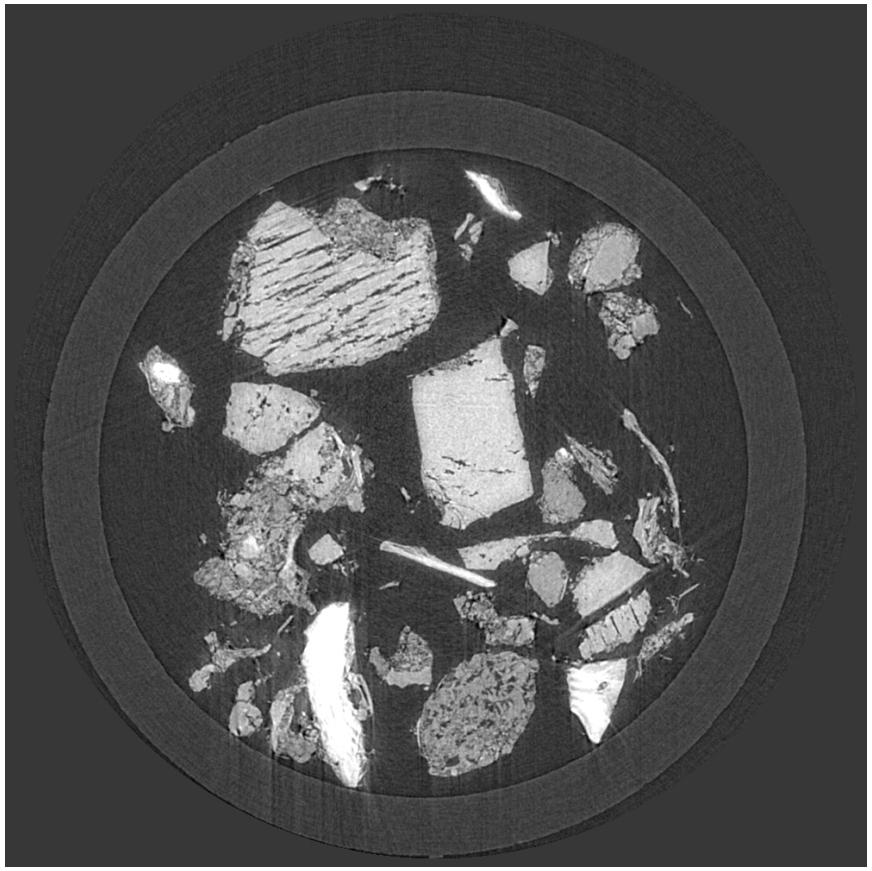

Masado (crushable sand)

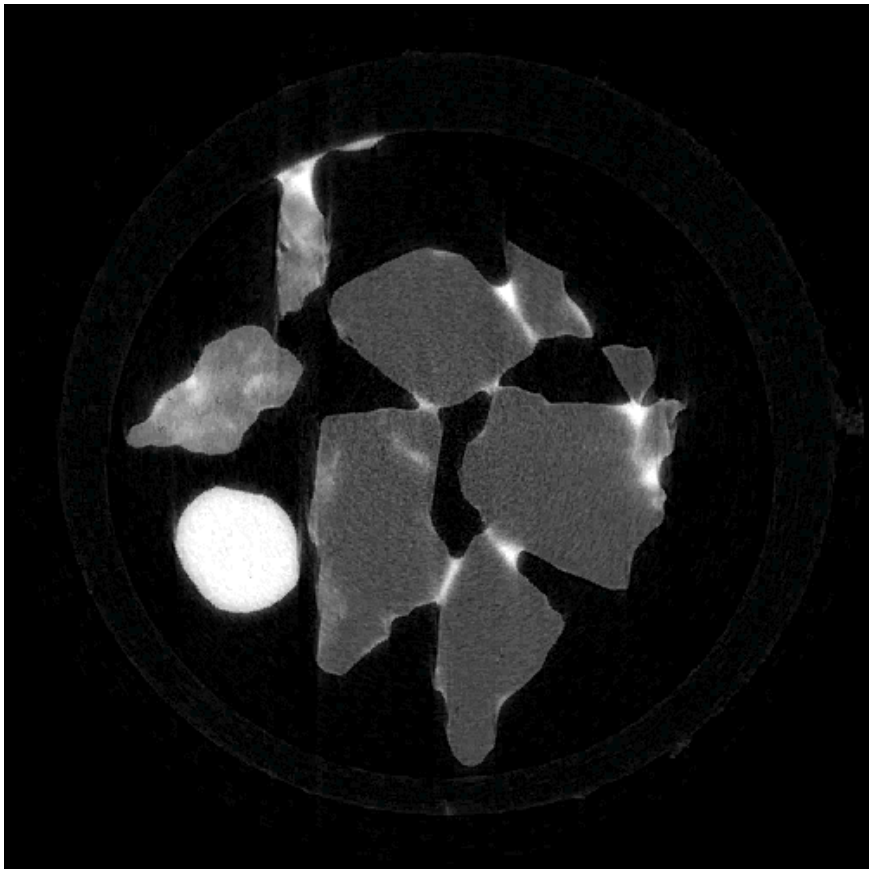

unsaturated condition

Micro Triaxial test (BL20B2)(1)

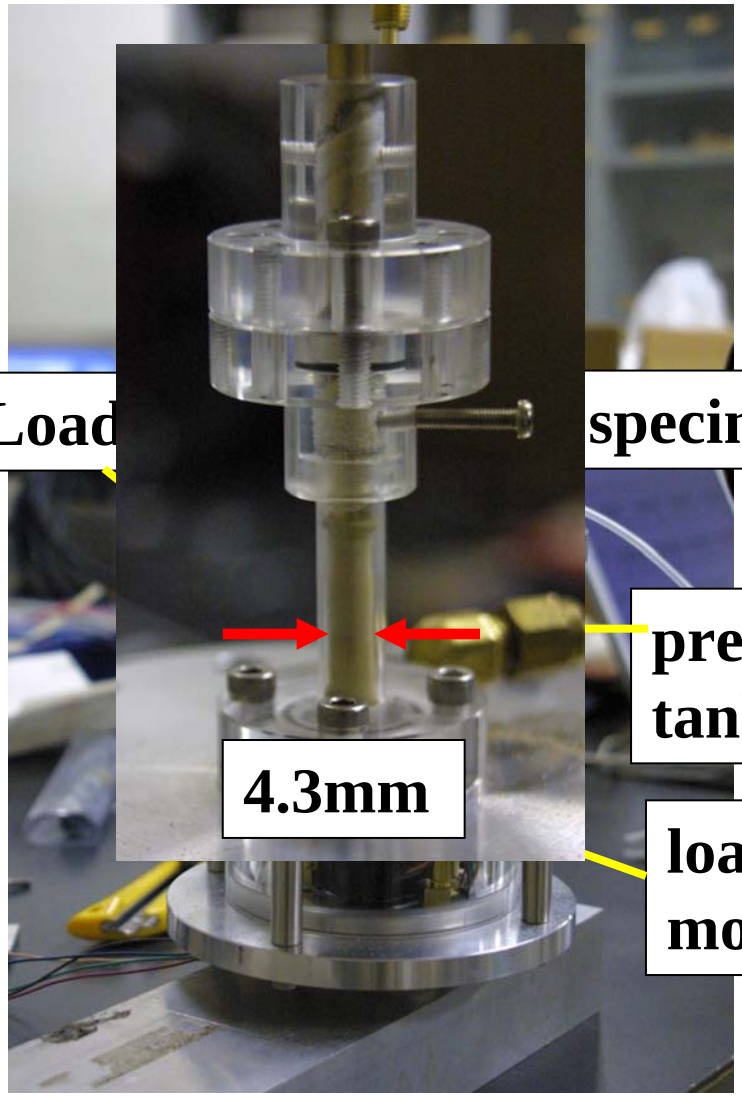

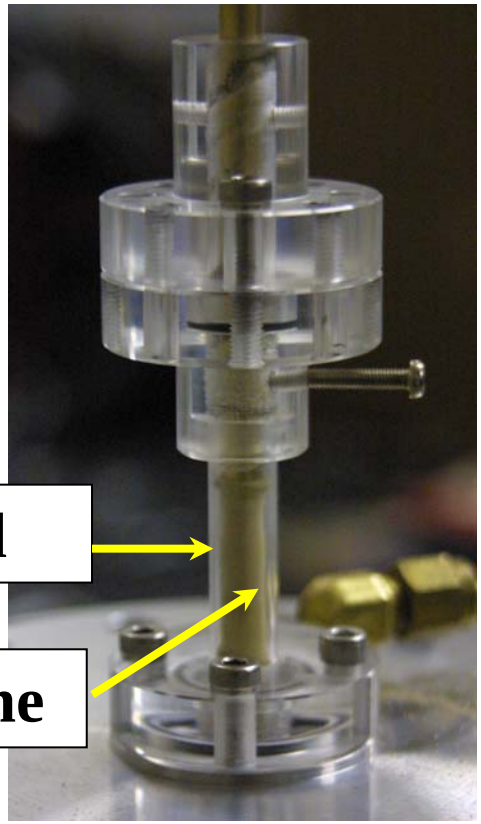

specimen	
diameter	4.3mm
height	10mm

Micro Triaxial test (BL20B2)(2)

CT scan of initial condition

↓

loading ←

↓

stop loading and CT scan (1.5 hours)

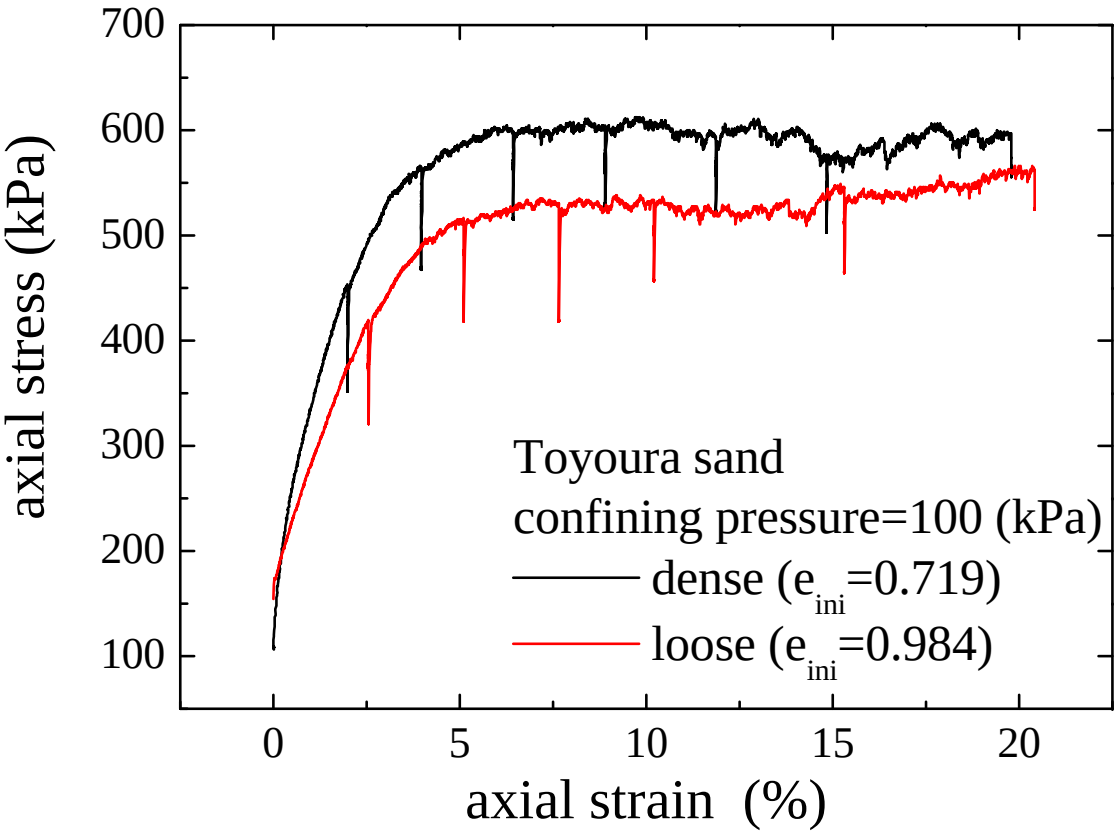

stress-strain curve

Micro Triaxial test (BL20B2)(3)

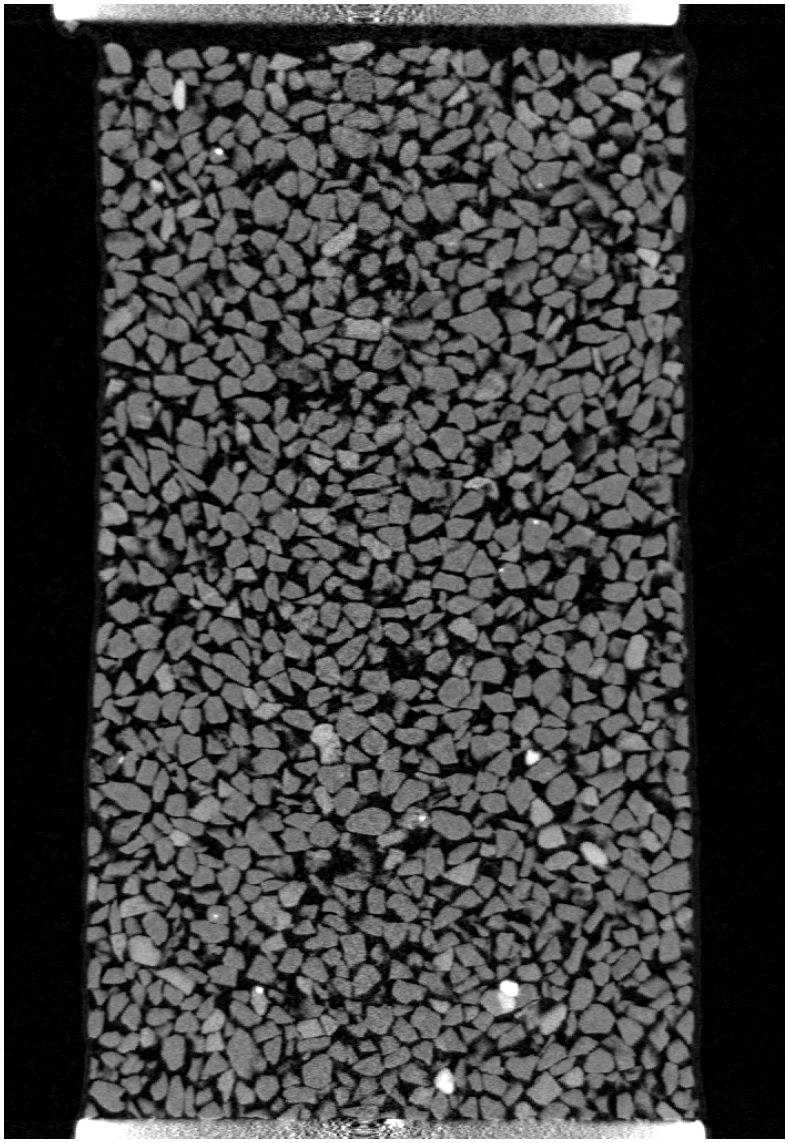

Toyoura
(medium dense)

void increase within
a shear band

Micro Triaxial test (BL20B2)(4)

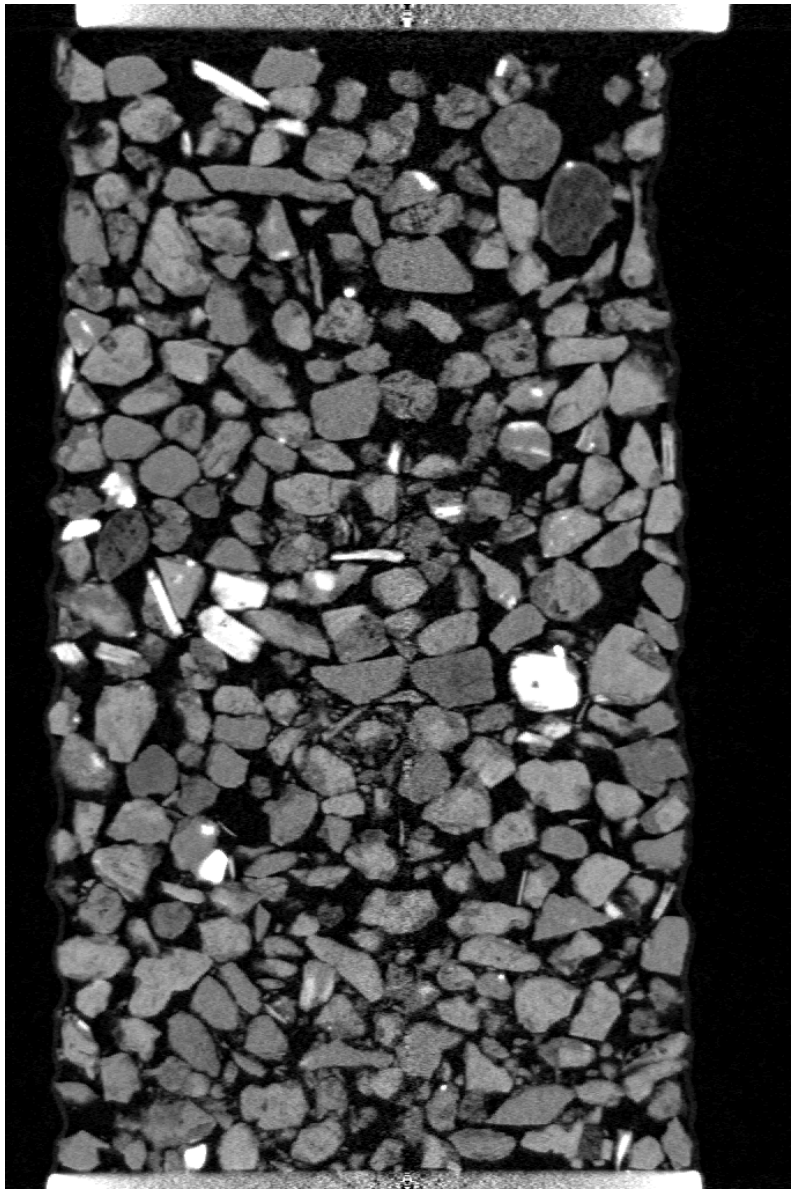

Masado (cruchable sand)
0.351-0.64mm
(medium dense)

particle crushing is
NOT predominant

Micro 1-D compression test

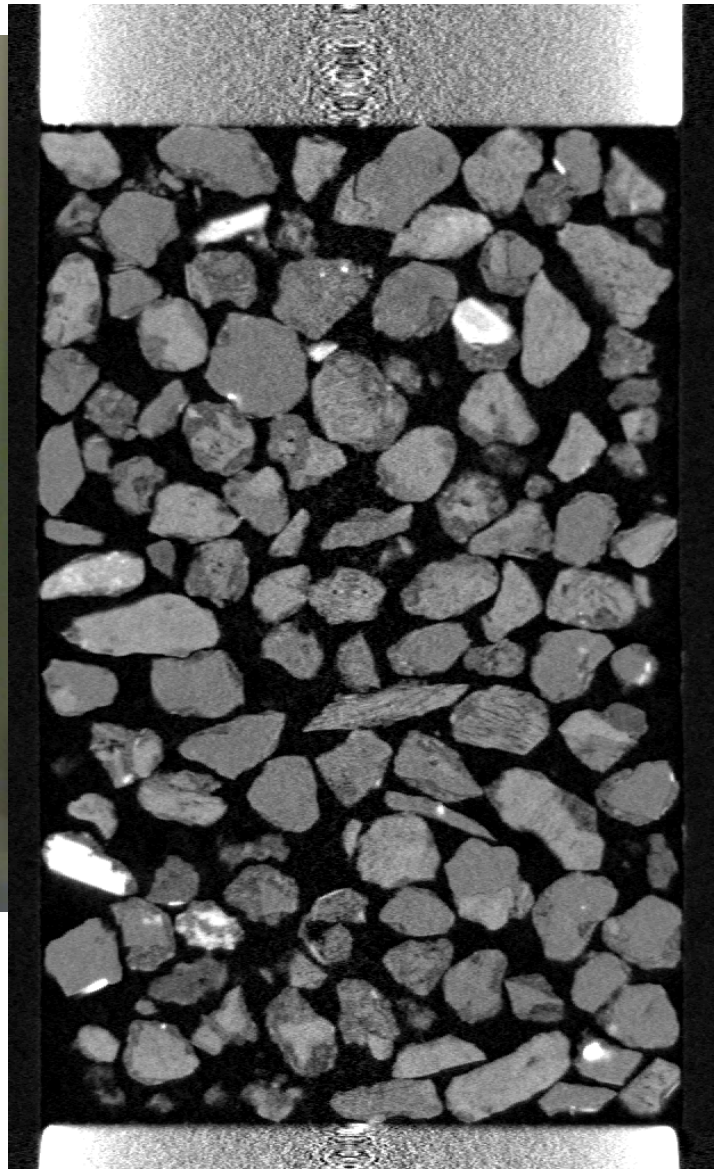

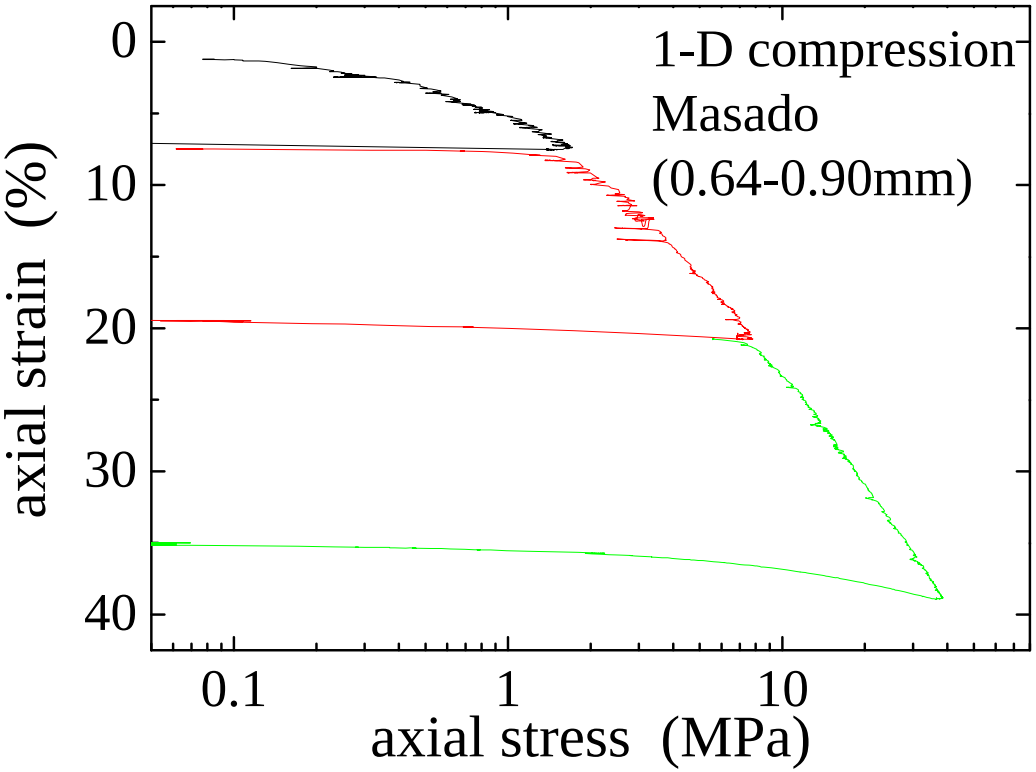

particle crushing after yield stress

Processing of CT image

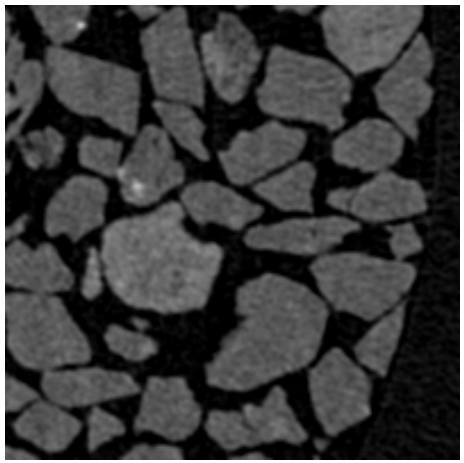

Original image

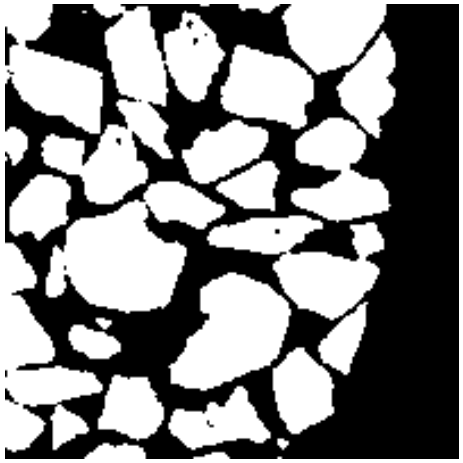

After binarization

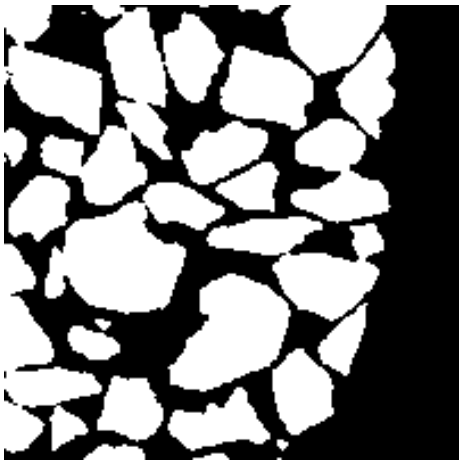

After pore-filling

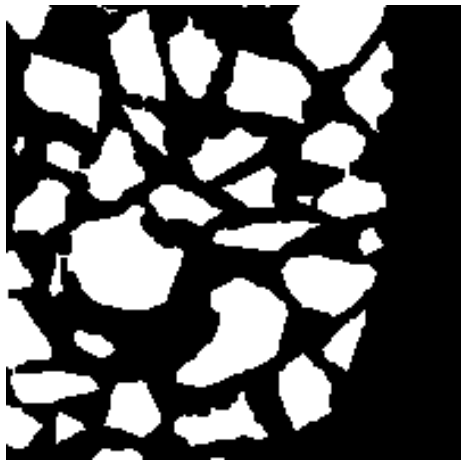

After 1st erosion

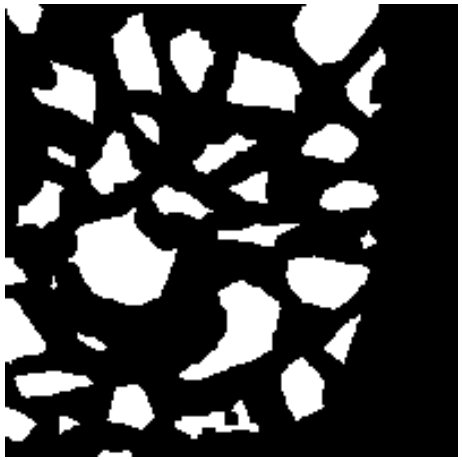

After 2nd erosion

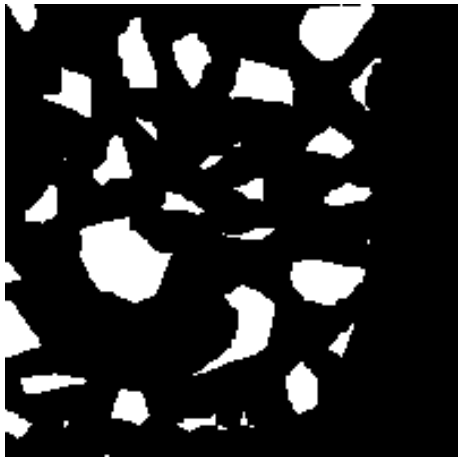

After 3rd erosion

Cluster labeling

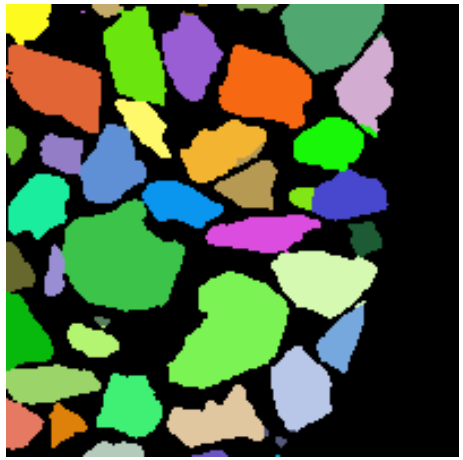

Attribution

Adequate erosion cycles

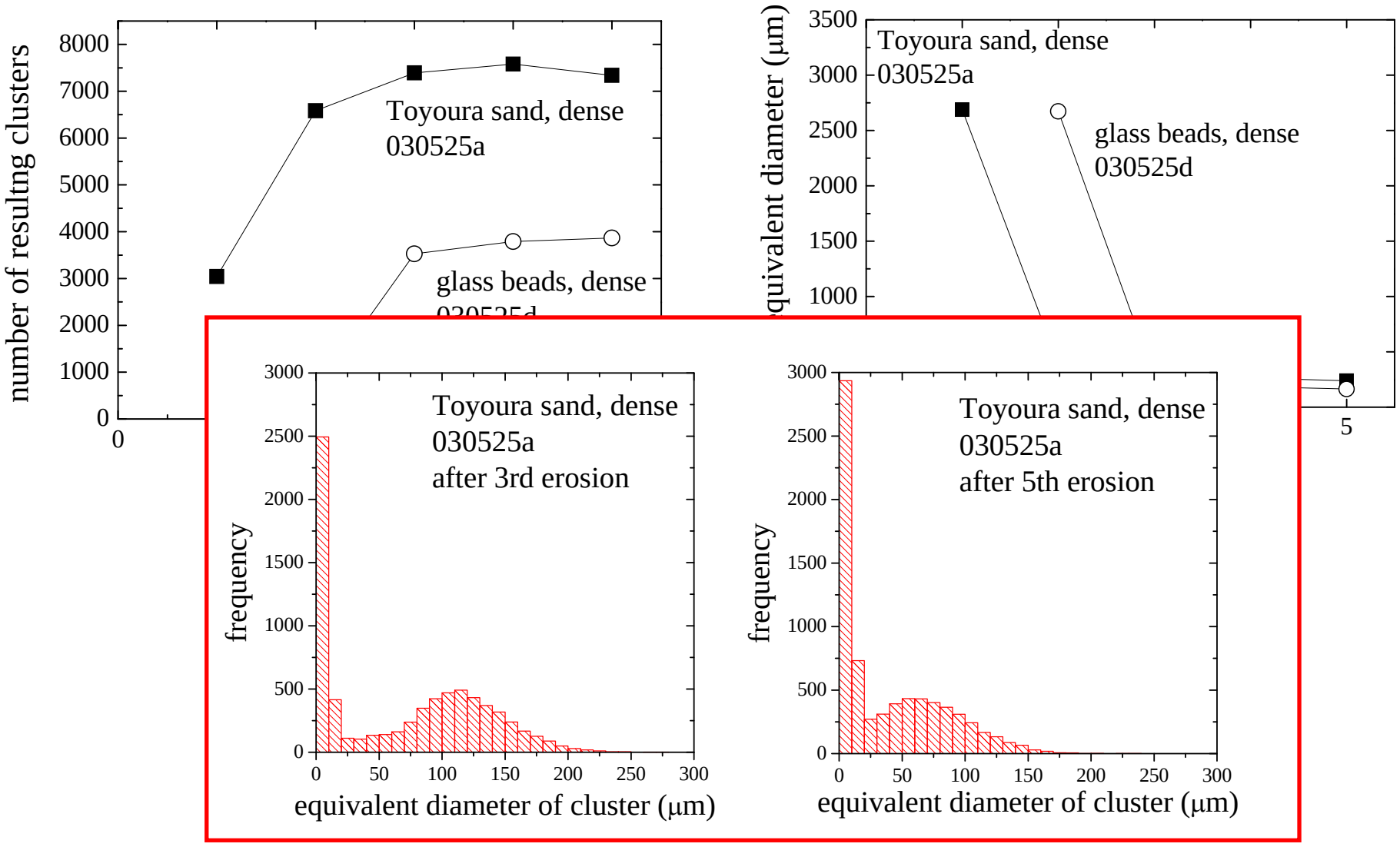

Grain identification

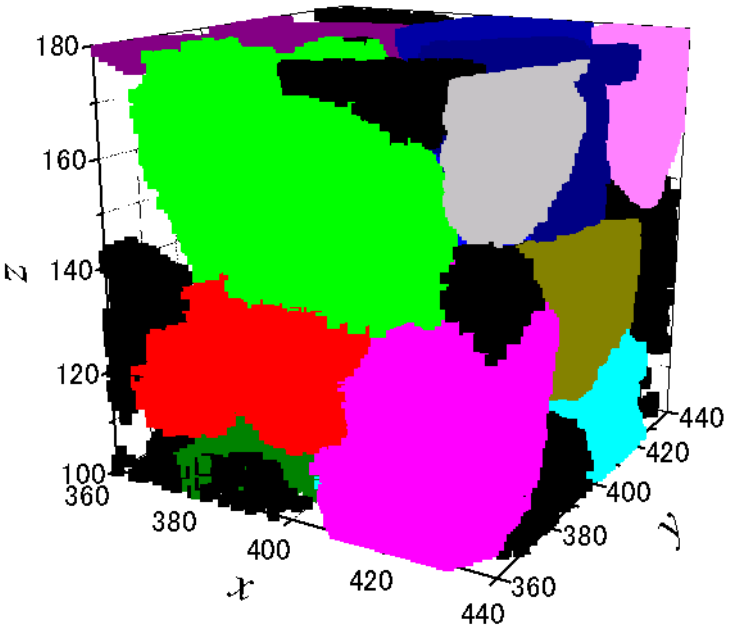

3-D image after attribution process

Grain identification

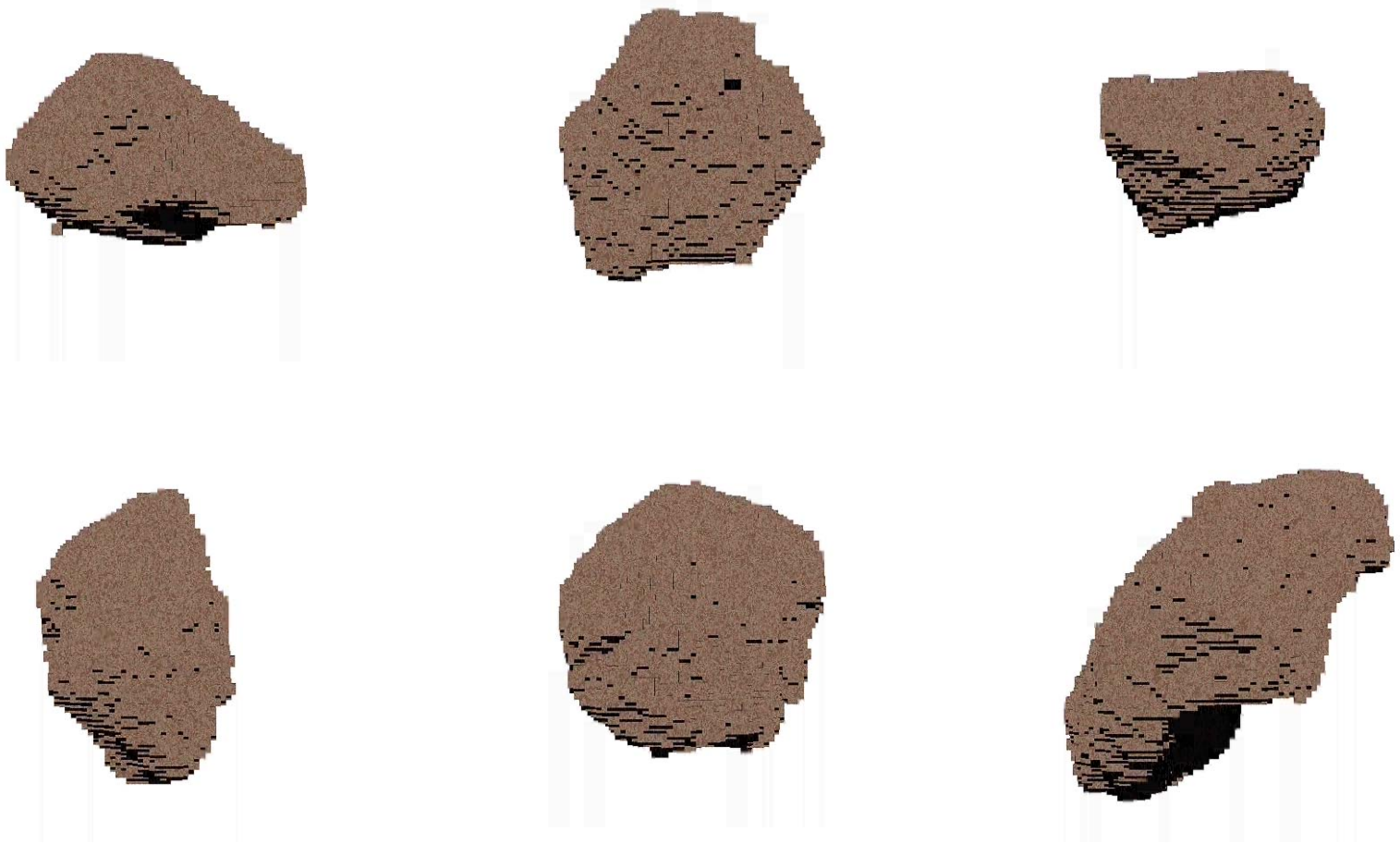

Identified Toyoura sand grains

Grain size distribution

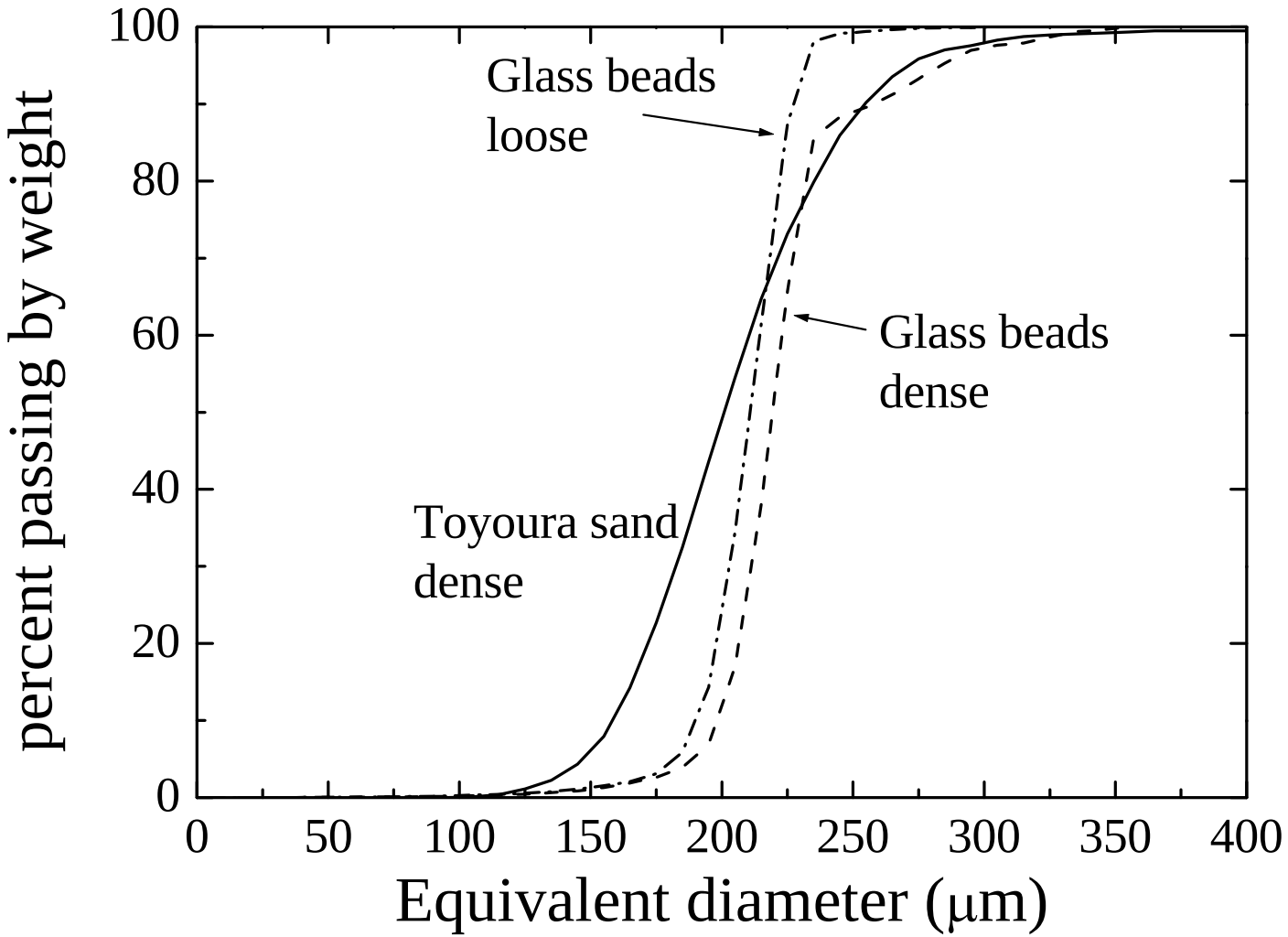

Contact area and their normals

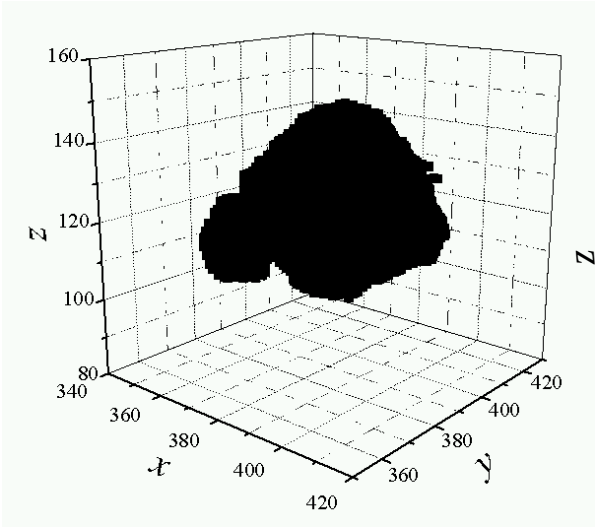

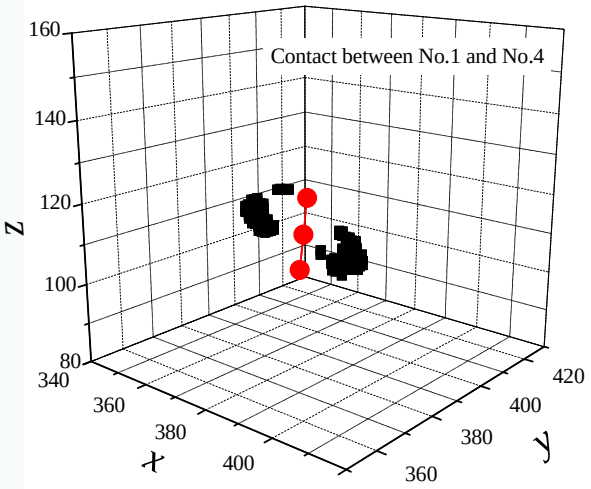

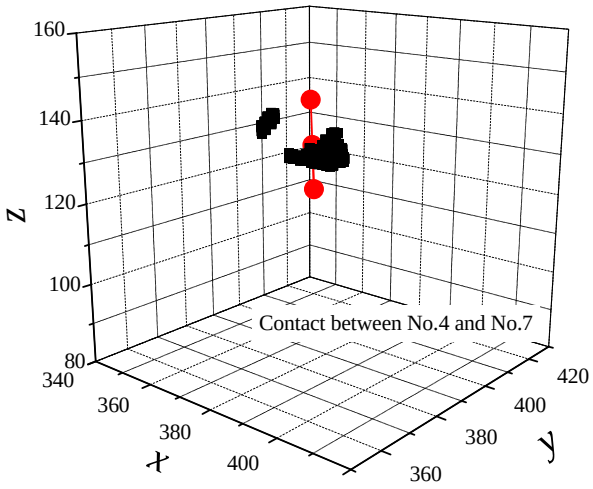

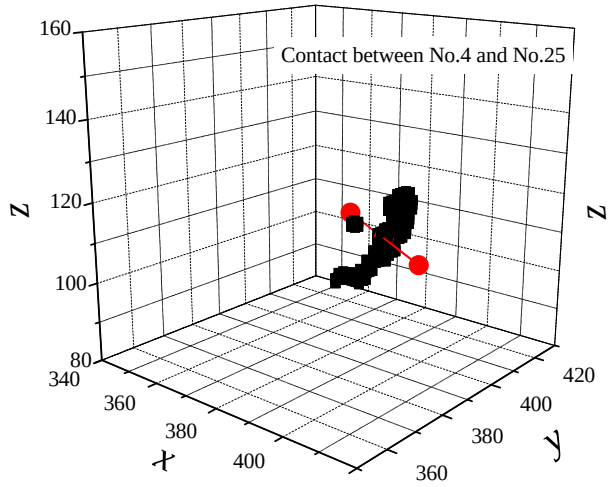

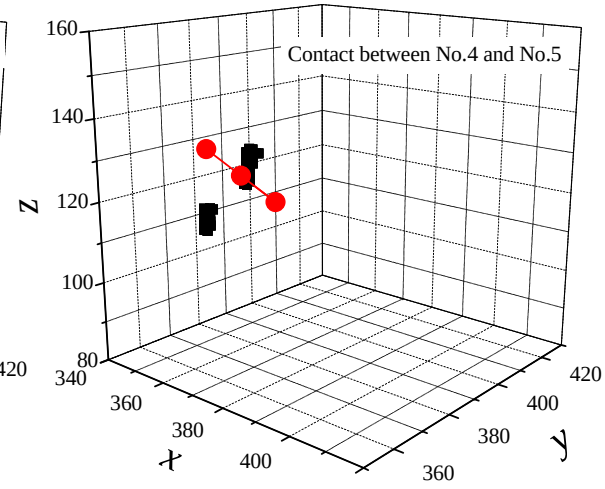

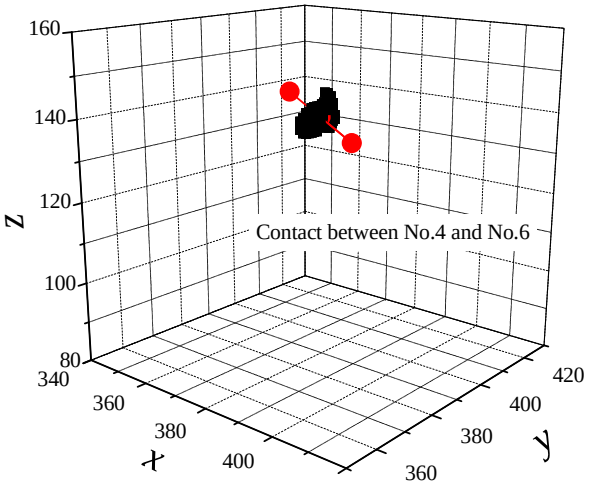

→ coordination number, fabric tensor, etc.

Coordination number (1)

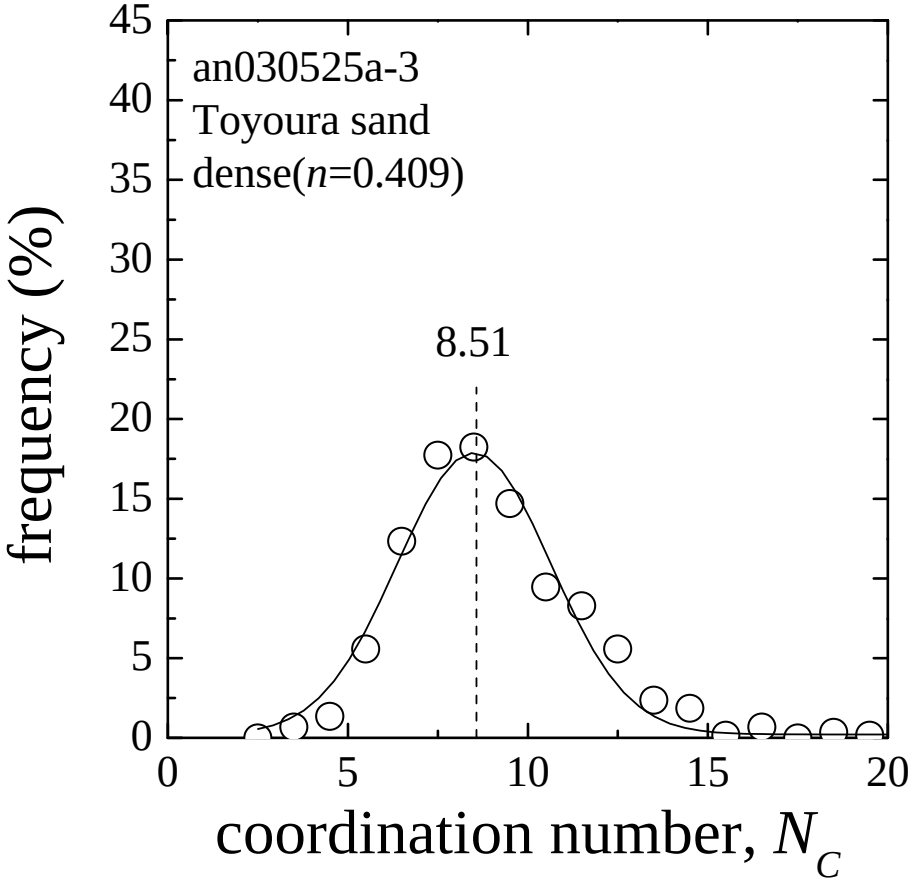

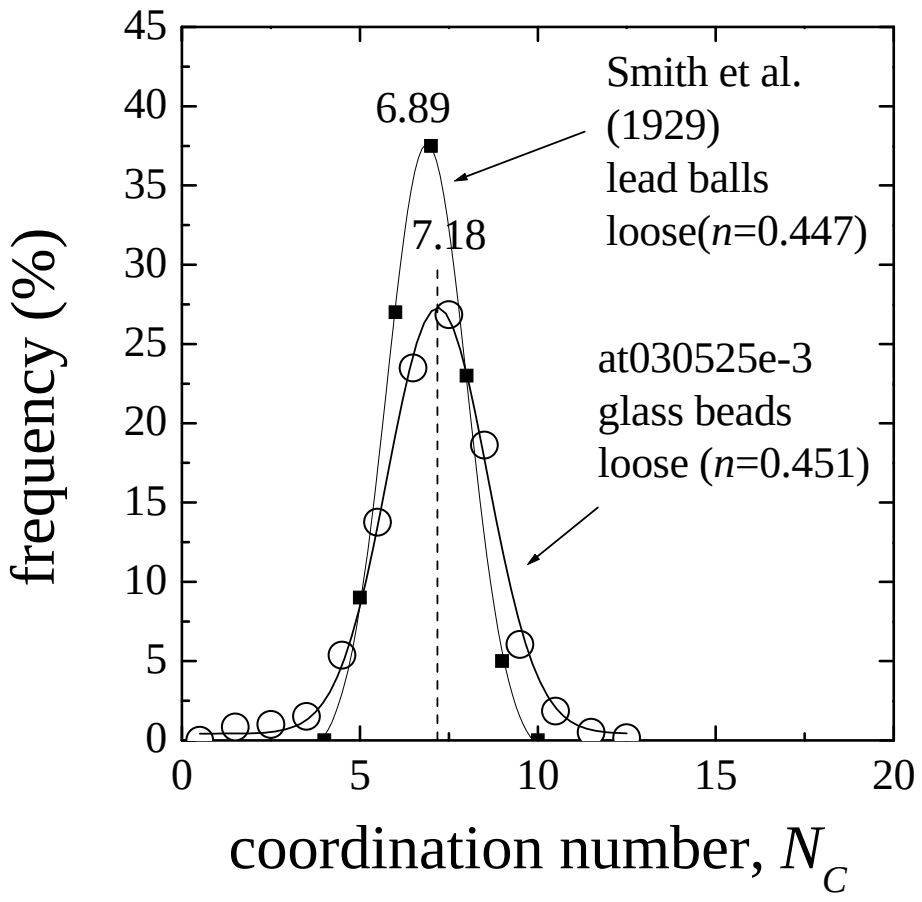

like a normal distribution

Coordination number (2)

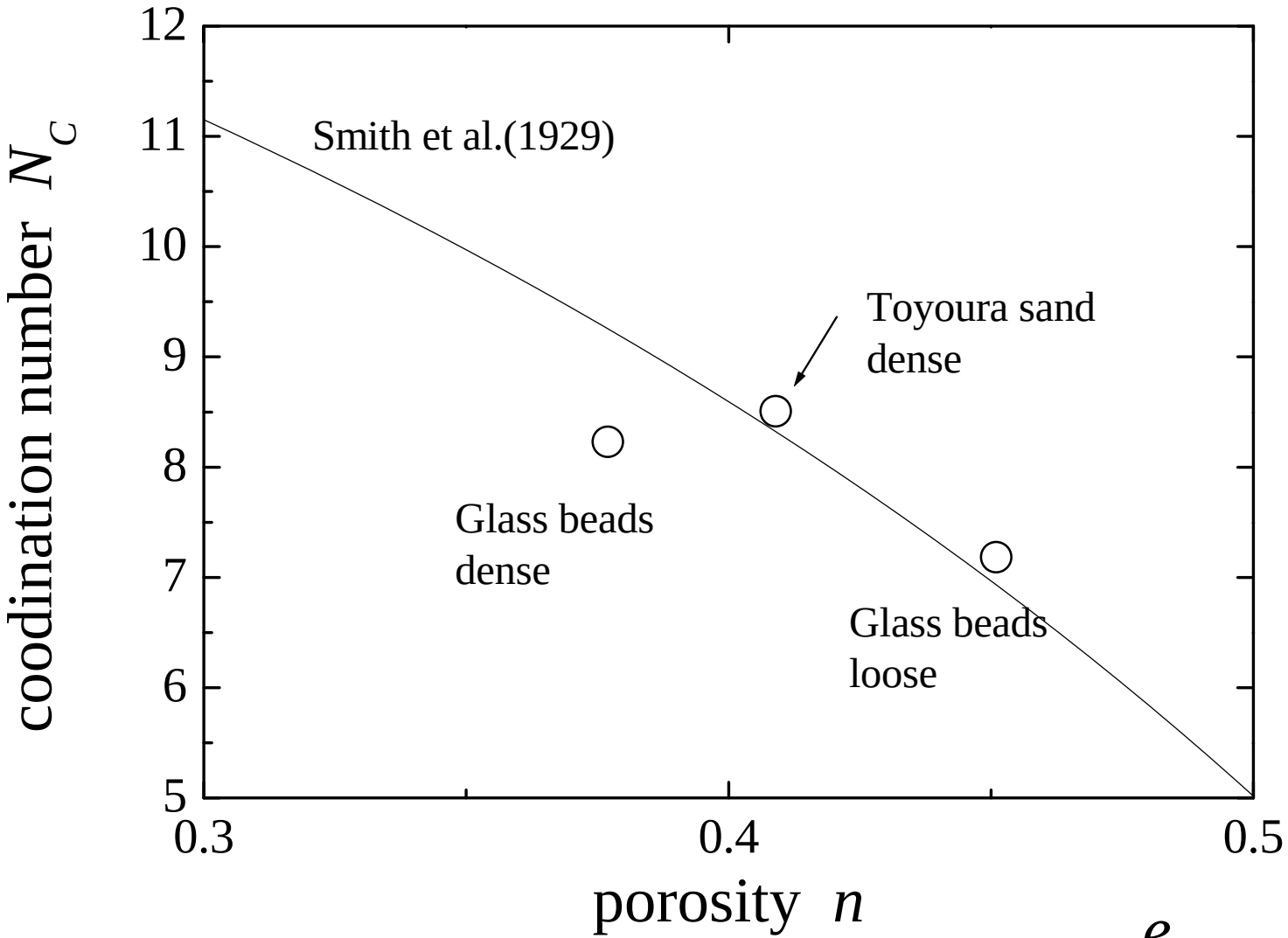

$$n = \frac{e}{e+1}$$

Next step

***Detection of each grain motion (translation and rotation)**

(Chang, Matsushima, Lee, J. Eng. Mech. ASCE, 2002.)

***Detection of grain crushing**

Image-based DEM

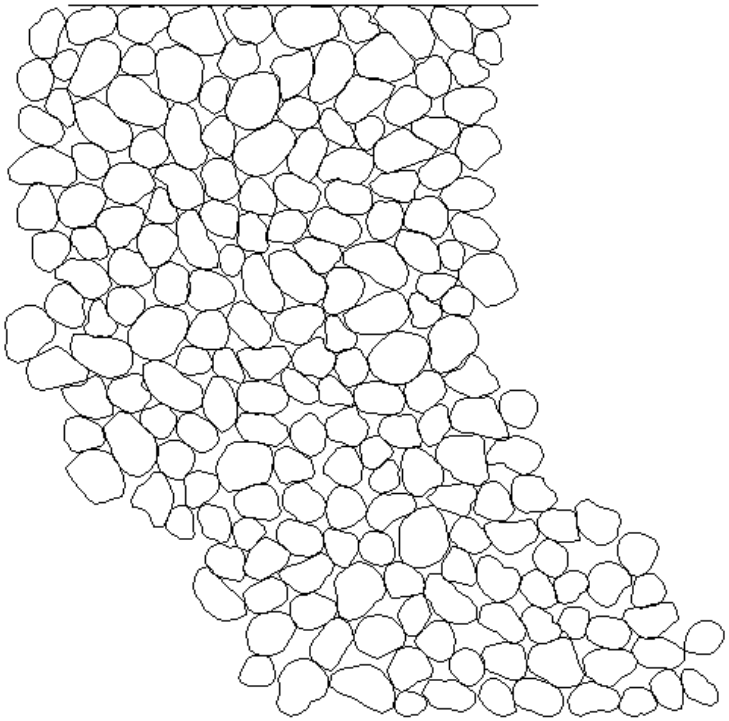

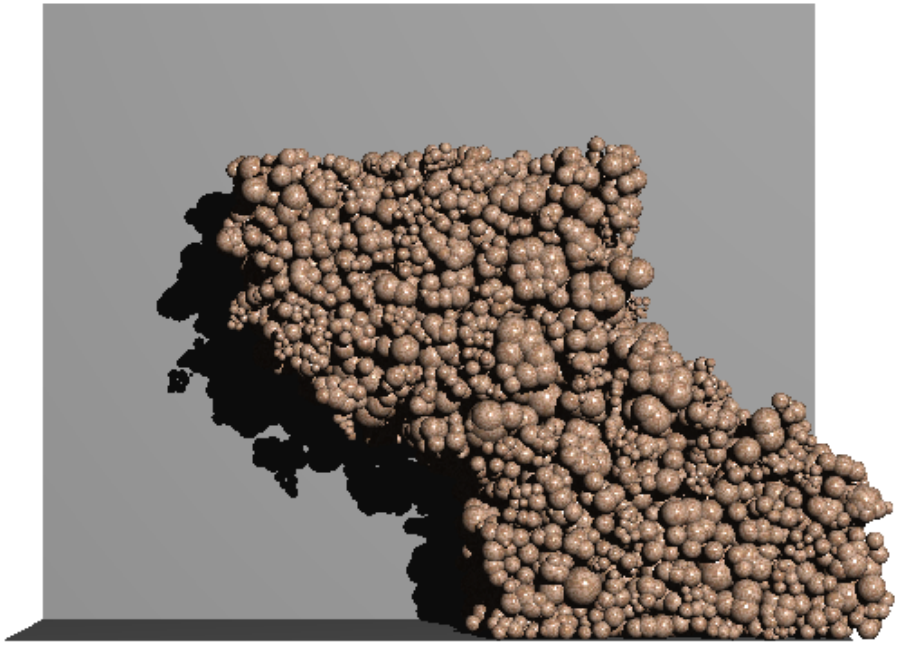

Background

* Rapid increase of computer abilities

→DEM simulations with large number of grains

* For quantitative discussion…

→Precise modeling of grains

(contact model, grain shape, crushability, etc.) is necessary.

This study deals with

GRAIN SHAPE MODELING

Image-based modeling (Matsushima and Saomoto 2002)

Irregular grain shape is described by a rigid connection of elements (circles or spheres)

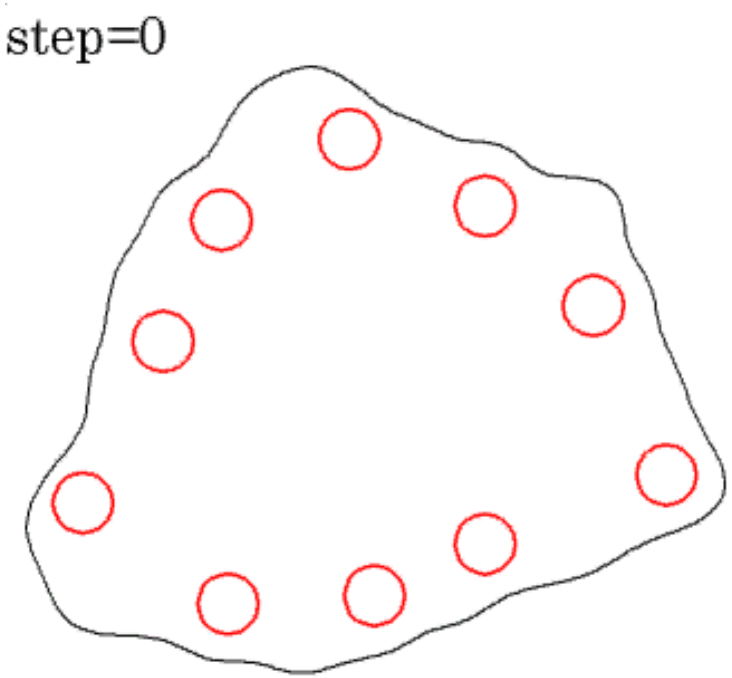

To find an optimum positions and radii of the elements…

time marching computation
(Dynamic optimization)

Each element moves and expands (or shrink) to get a better fitting to the target grain shape

Dynamic Optimization algorithm

Each surface point of a target grain gives an attraction to the closest element

which directs from the centroid of the element to the surface point

and its magnitude is proportional to the distance.

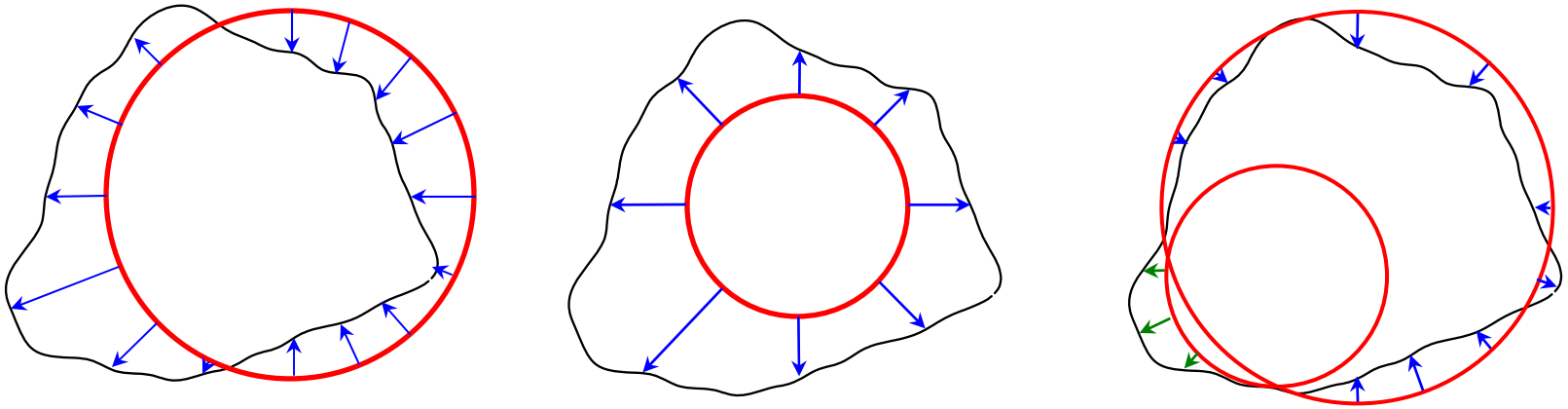

2D example (1)

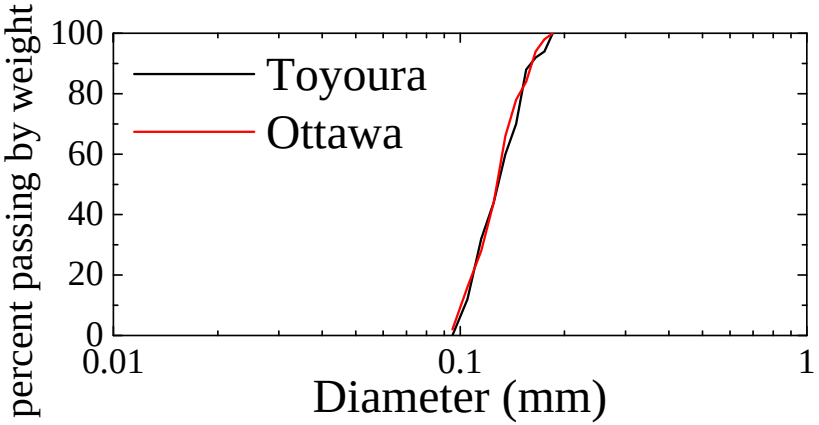

Grain density	2.64(g/cm^2)
Spring constant	
（normal）	1.0e9 (g/s^2)
（tangential）	2.5e8 (g/s^2)
Damping coefficient	
（normal）	2.0e2 (g/s)
（tangential）	1.0e2 (g/s)
Friction coefficient between grains	27 (deg.)
Time increment	2.5e-8 (sec.)

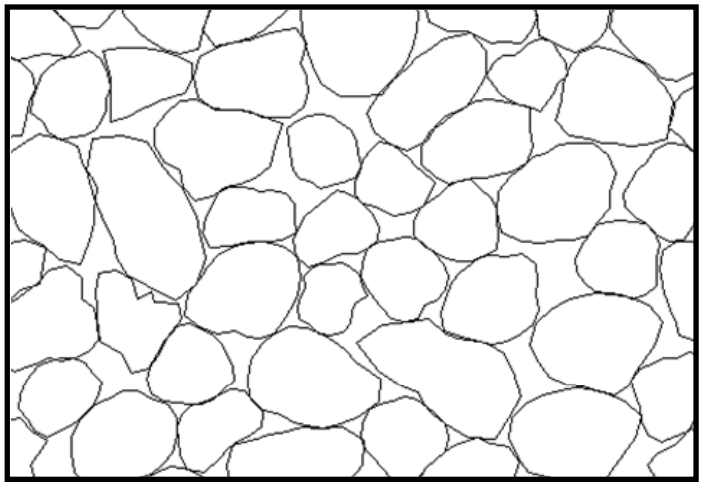

Toyoura sand (sub-angular)

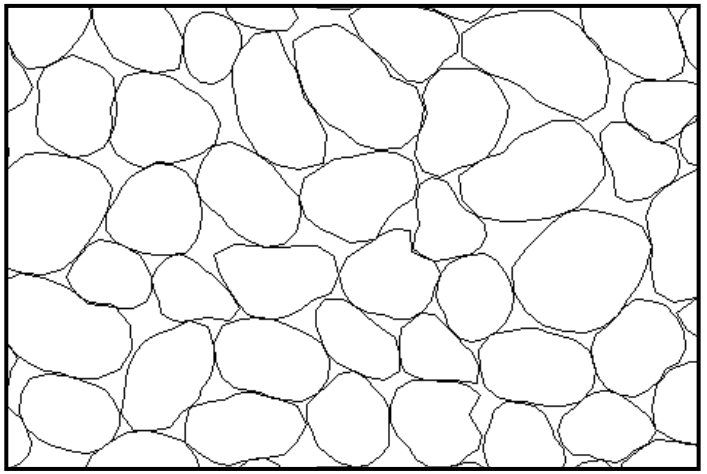

Ottawa sand (sub-rounded)

2D example (2)

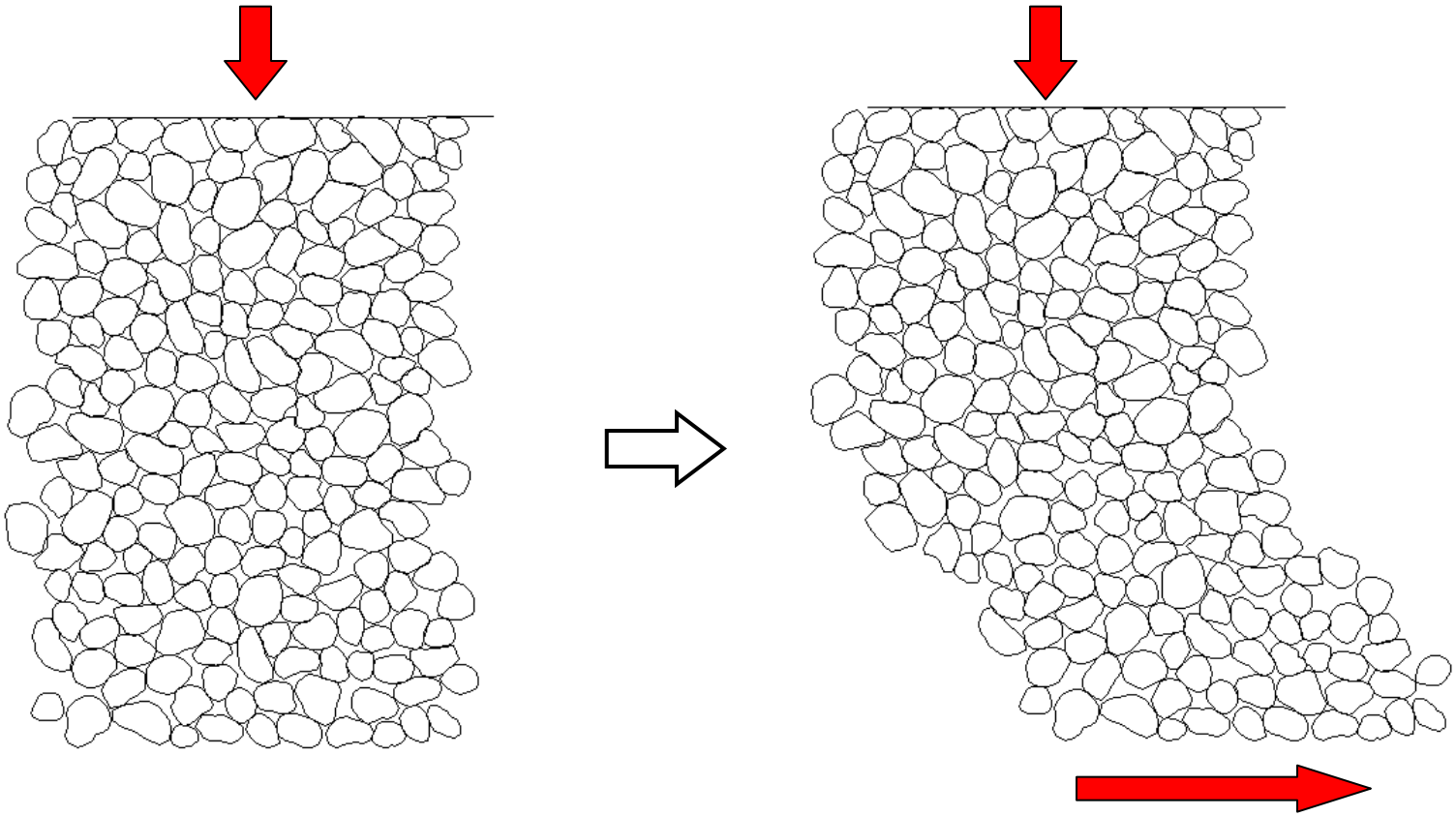

200 grains (Each grain is modeled with 10 elements)
Periodic boundary at both sides
Constant confining pressure(10kN/m),
Lateral displacement is imposed at the bottom grains

2D example (3)

Dense specimen (e_{ini}=0.20)

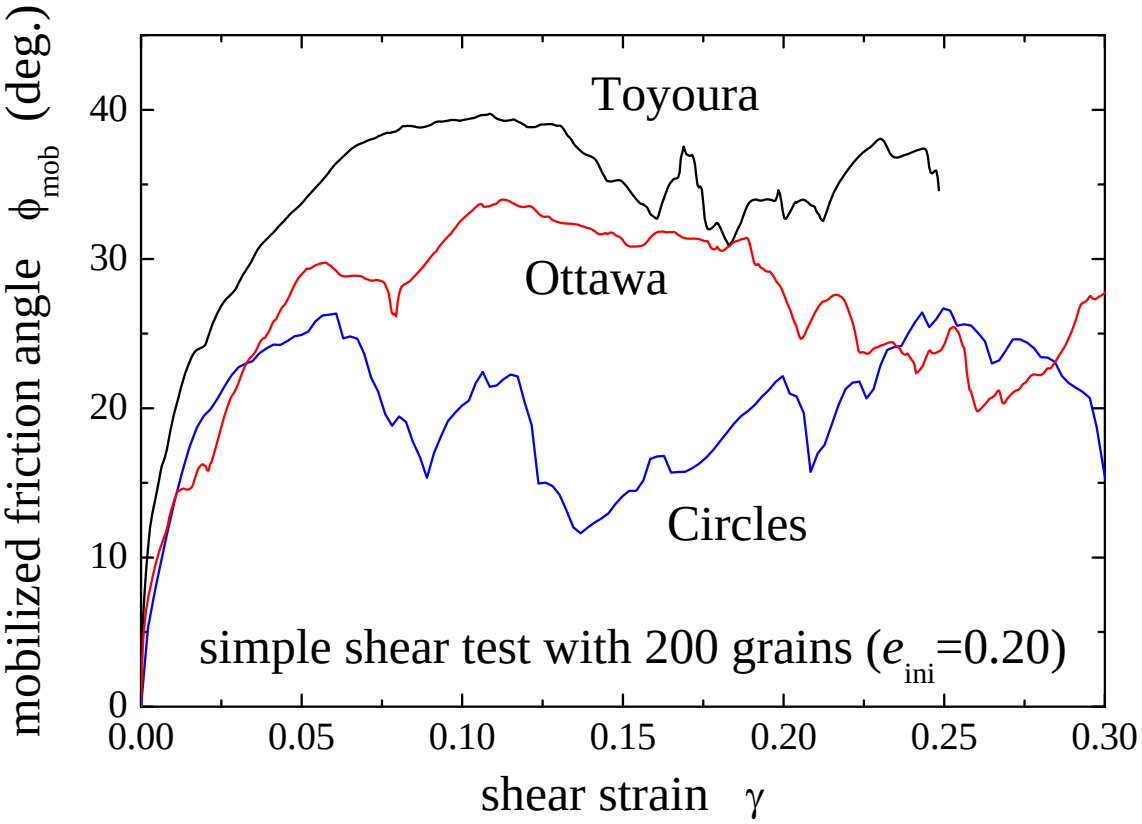

Toyoura>Ottawa>Circles for peak strength

2D example (4)

Peak strengths with different initial void ratio

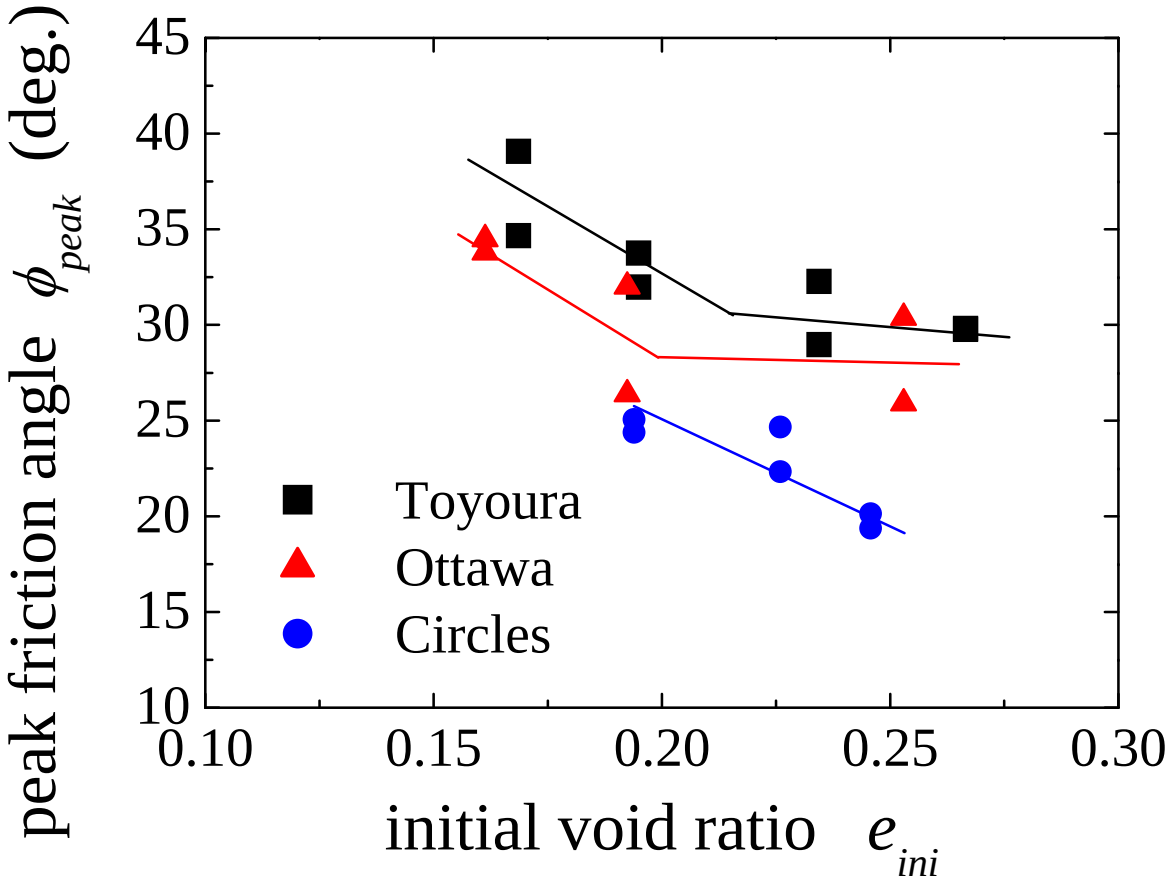

The modeling is verified qualitatively.

2D example (5)

Granular column structure during shear

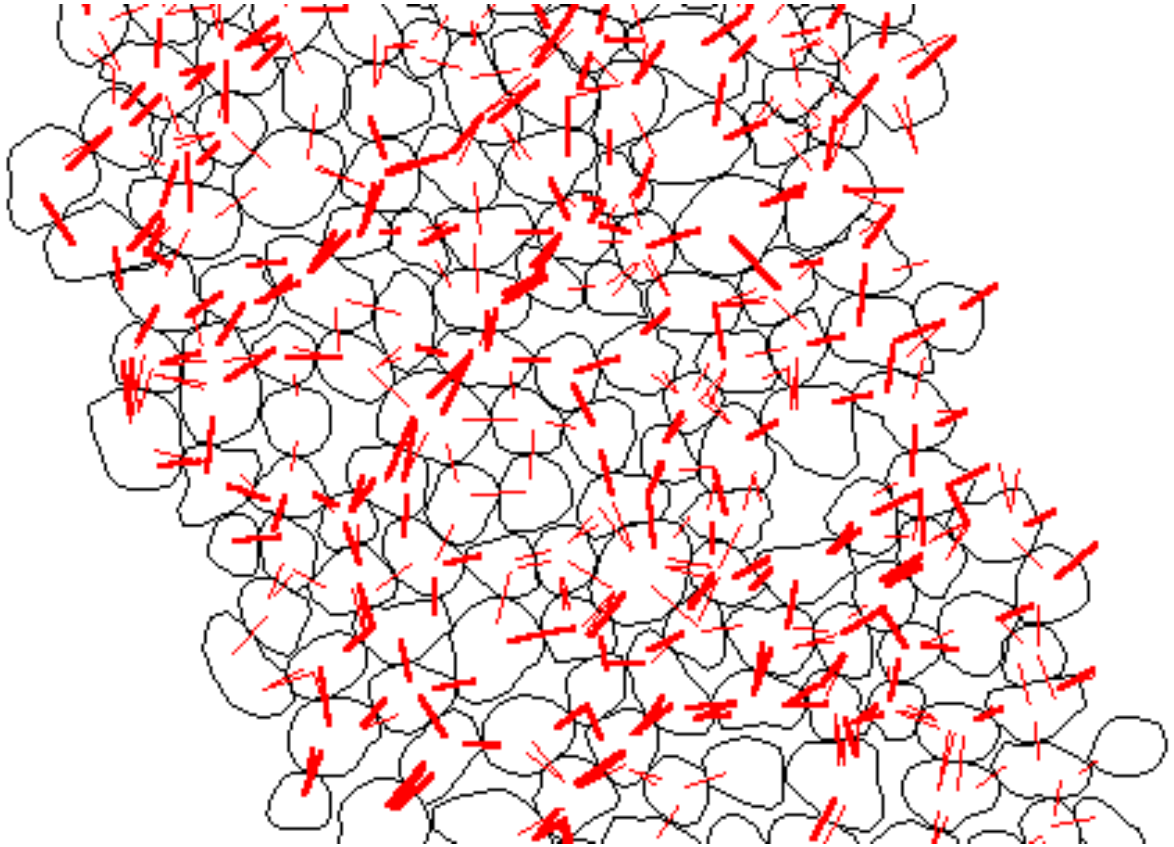

Two grains are in contact with plural points

→Moment transmission →Higher strength

3D example: Toyoura sand (1)

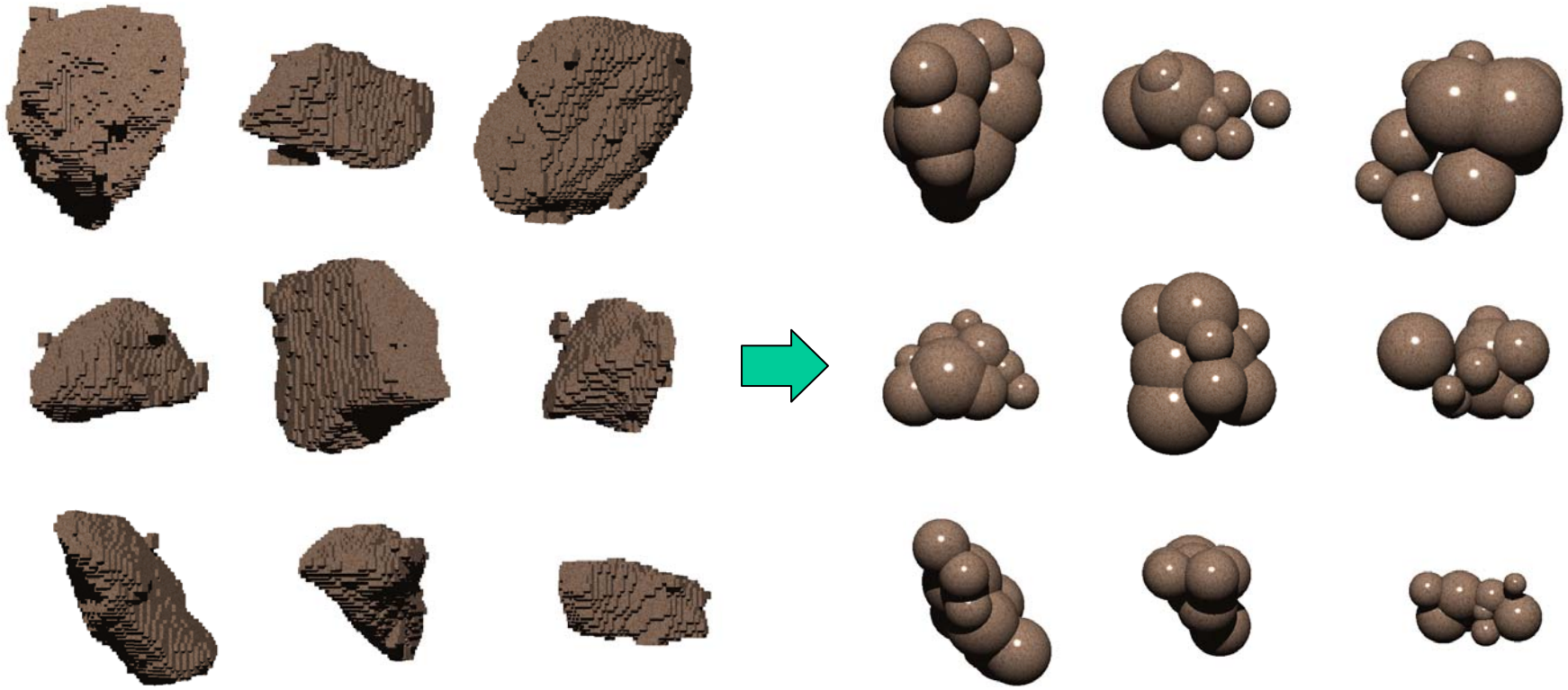

X-ray CT result **3D modeling**

Toyoura sand model

3D example: Toyoura sand (2)

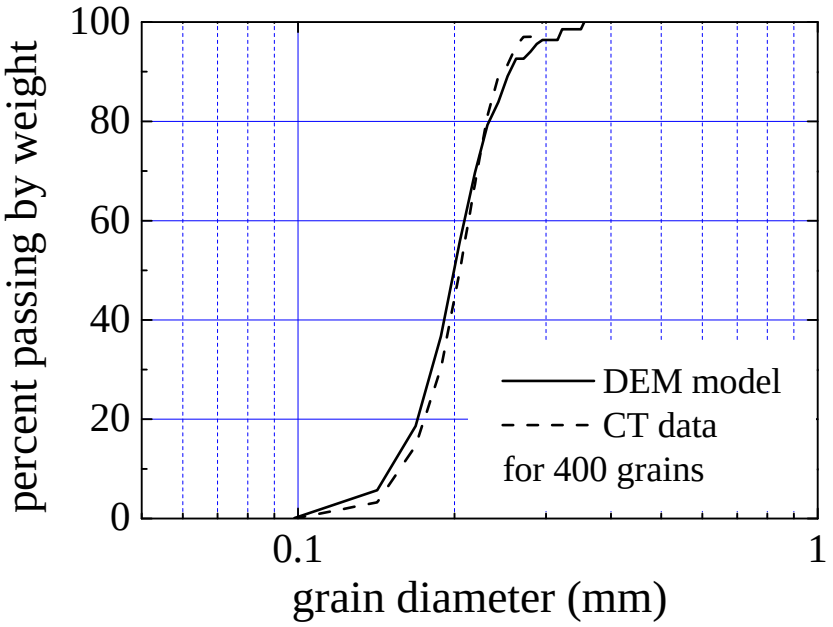

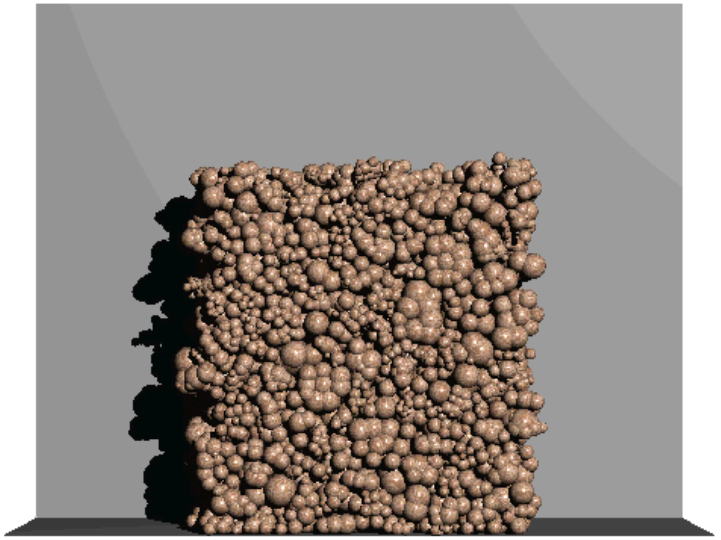

Grain size distribution:
DEM model = original CT data

Simple shear simulation

3D example: Toyoura sand (3)

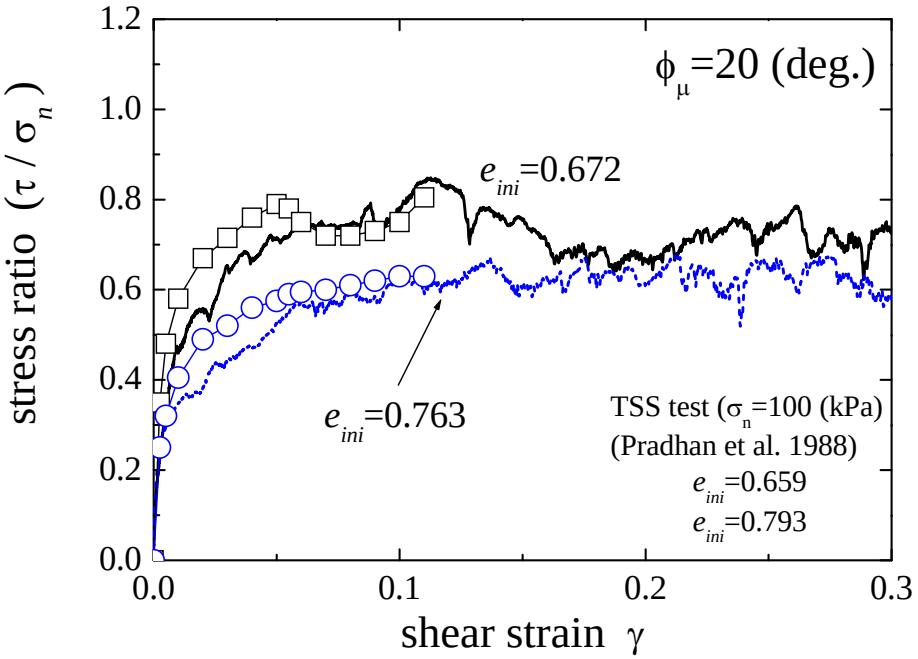

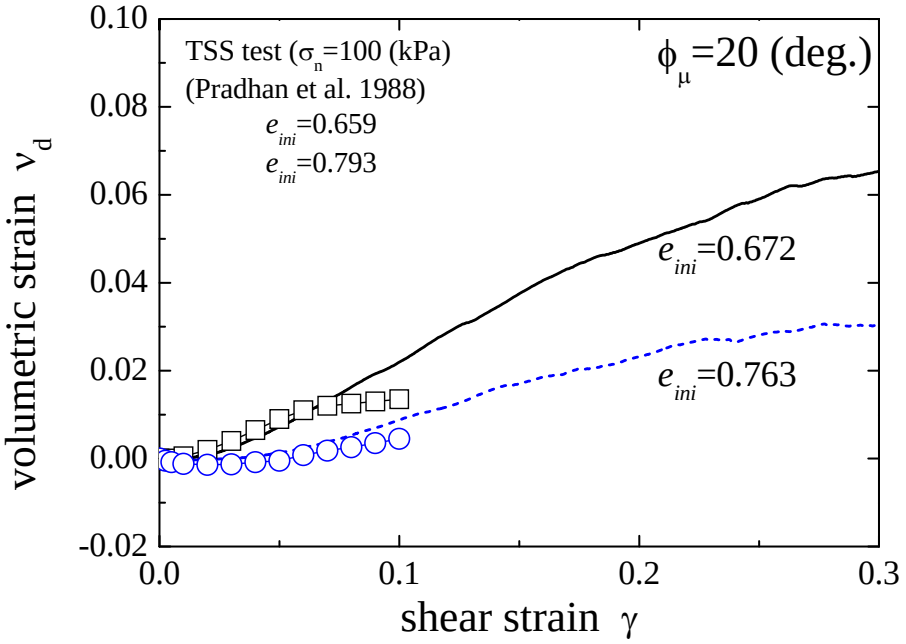

Stress-strain curve **dilation curve**

Quantitative agreement with experiment if inter-particle friction angle=20(deg.)

Matsushima 2004

3D example: Toyoura sand (4)

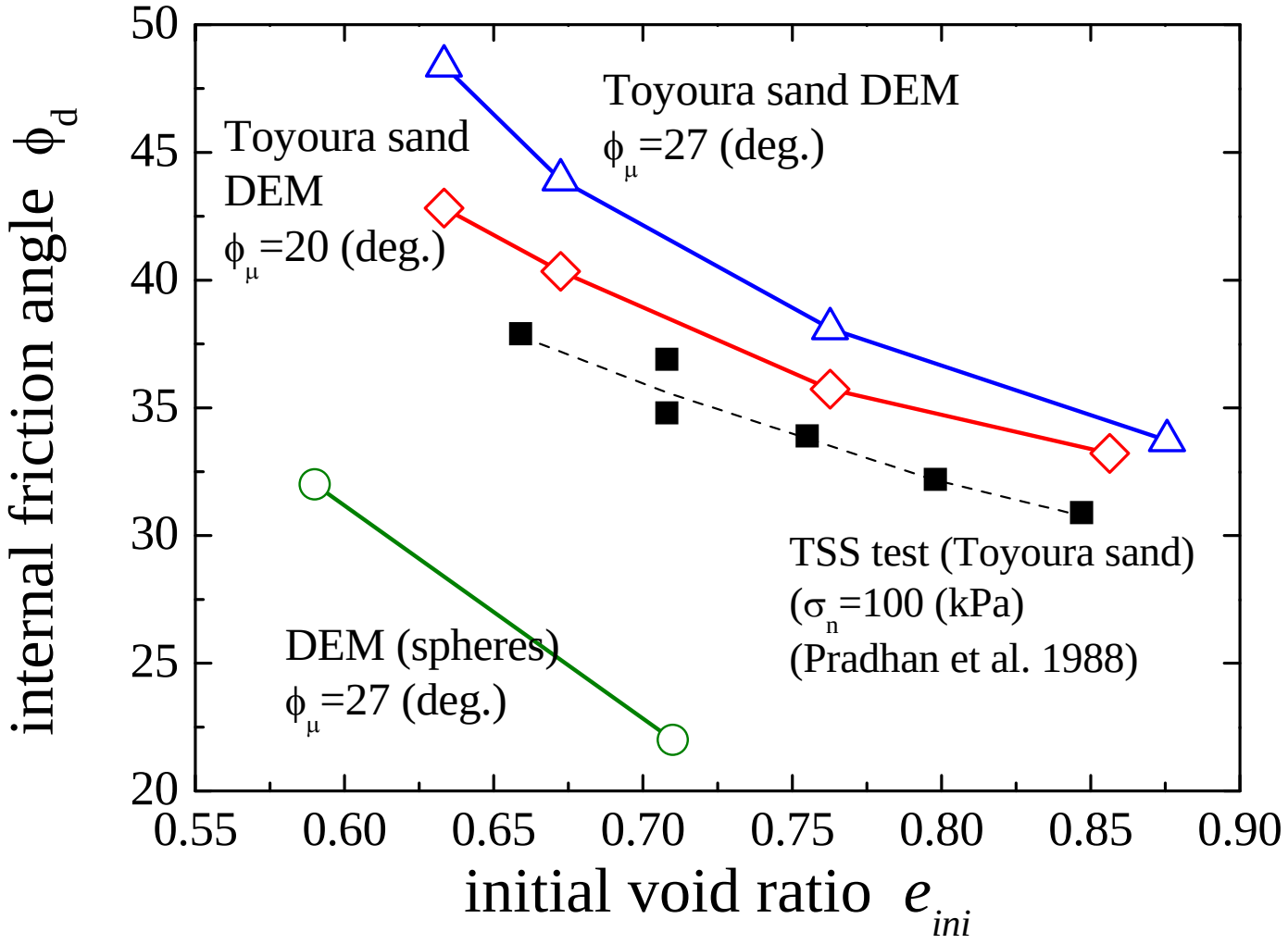

Peak strength for various void ratio

Lunar soil simulant (1)

600 grains (10-spheres model) are fell down into a vessel

Periodic boundary in y-direction

Bottom grains are fixed into the bottom plate

Remove the right side wall

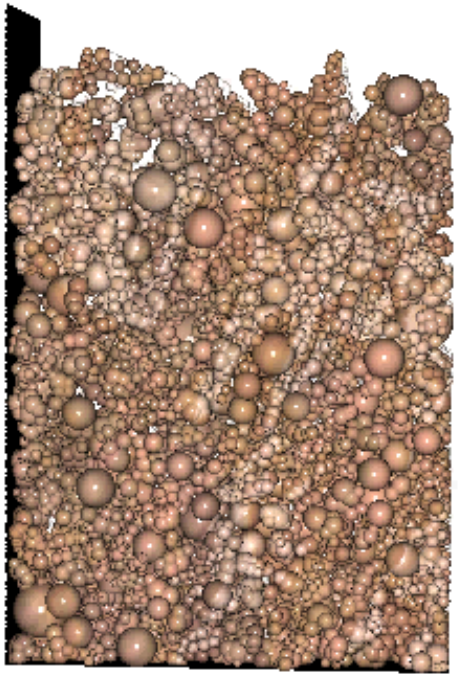

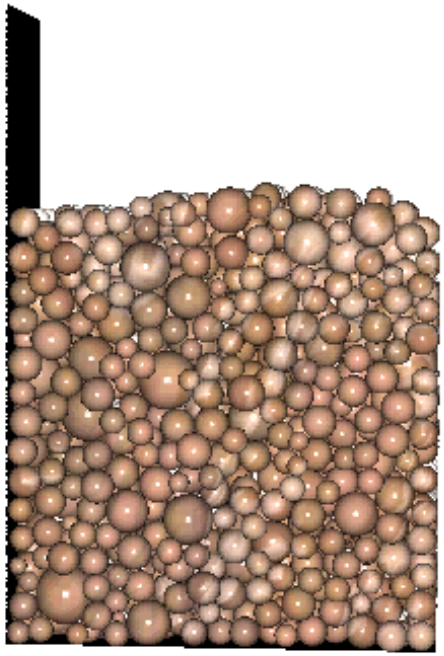

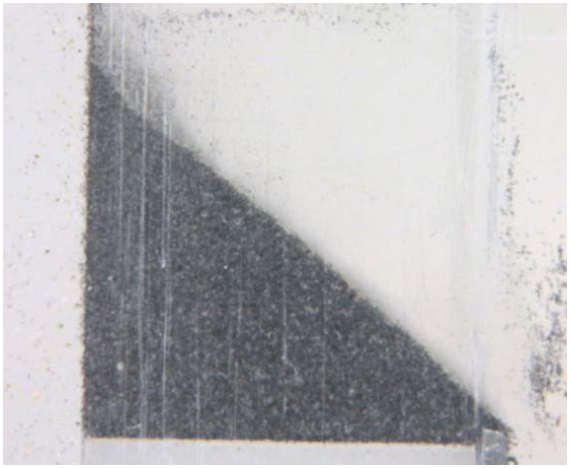

Lunar soil simulant(3): Parametric study

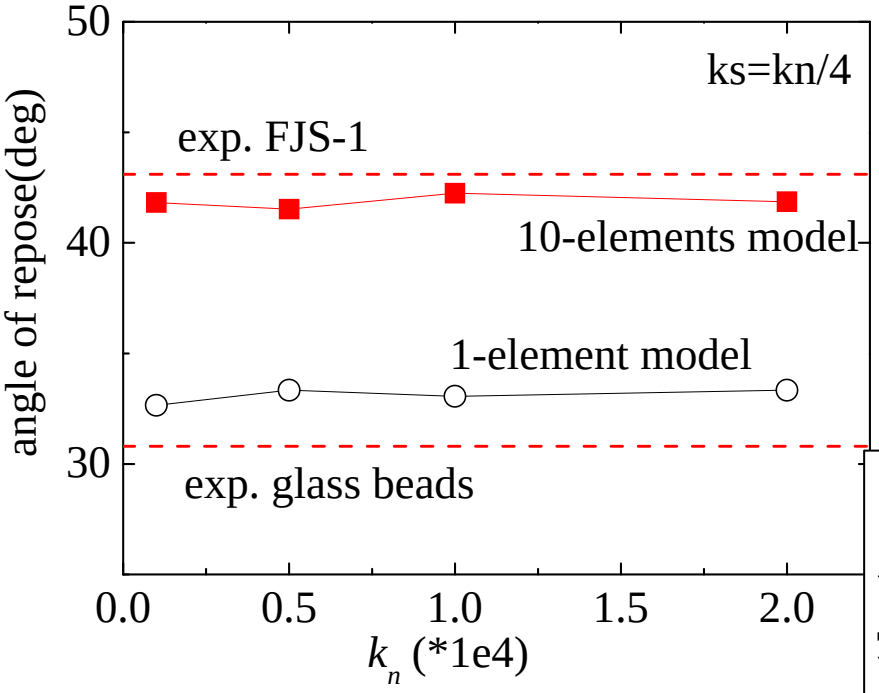

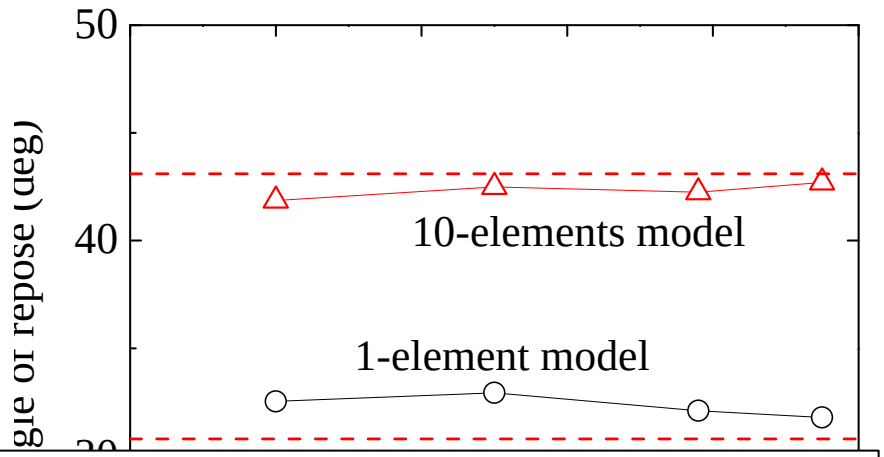

Effect of grain hardness

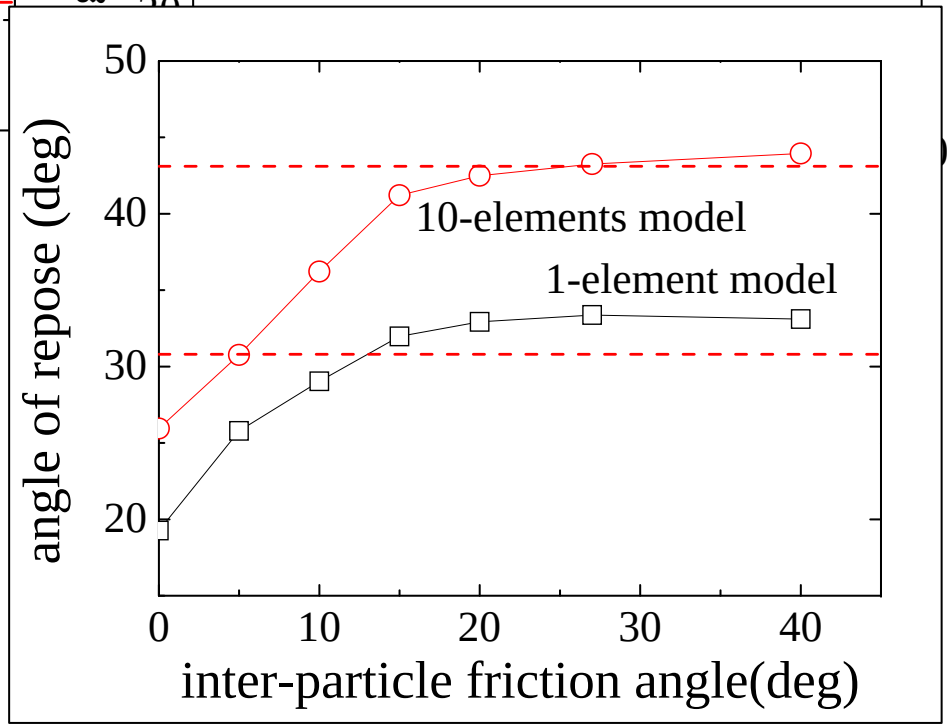

effect of interparticle friction

Lunar soil simulant(4): model accuracy

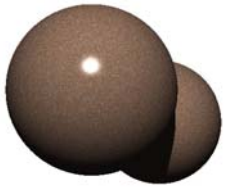

2-elements model

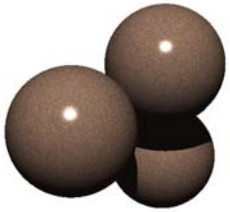

3-elements model

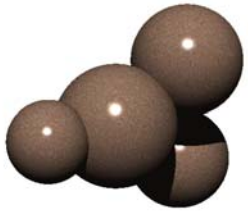

4-elements model

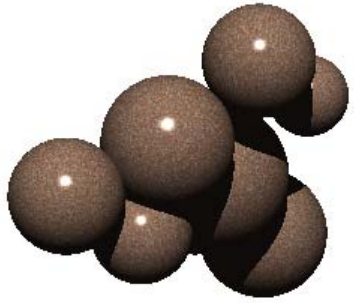

7-elements model

Lunar soil simulant(5): model accuracy

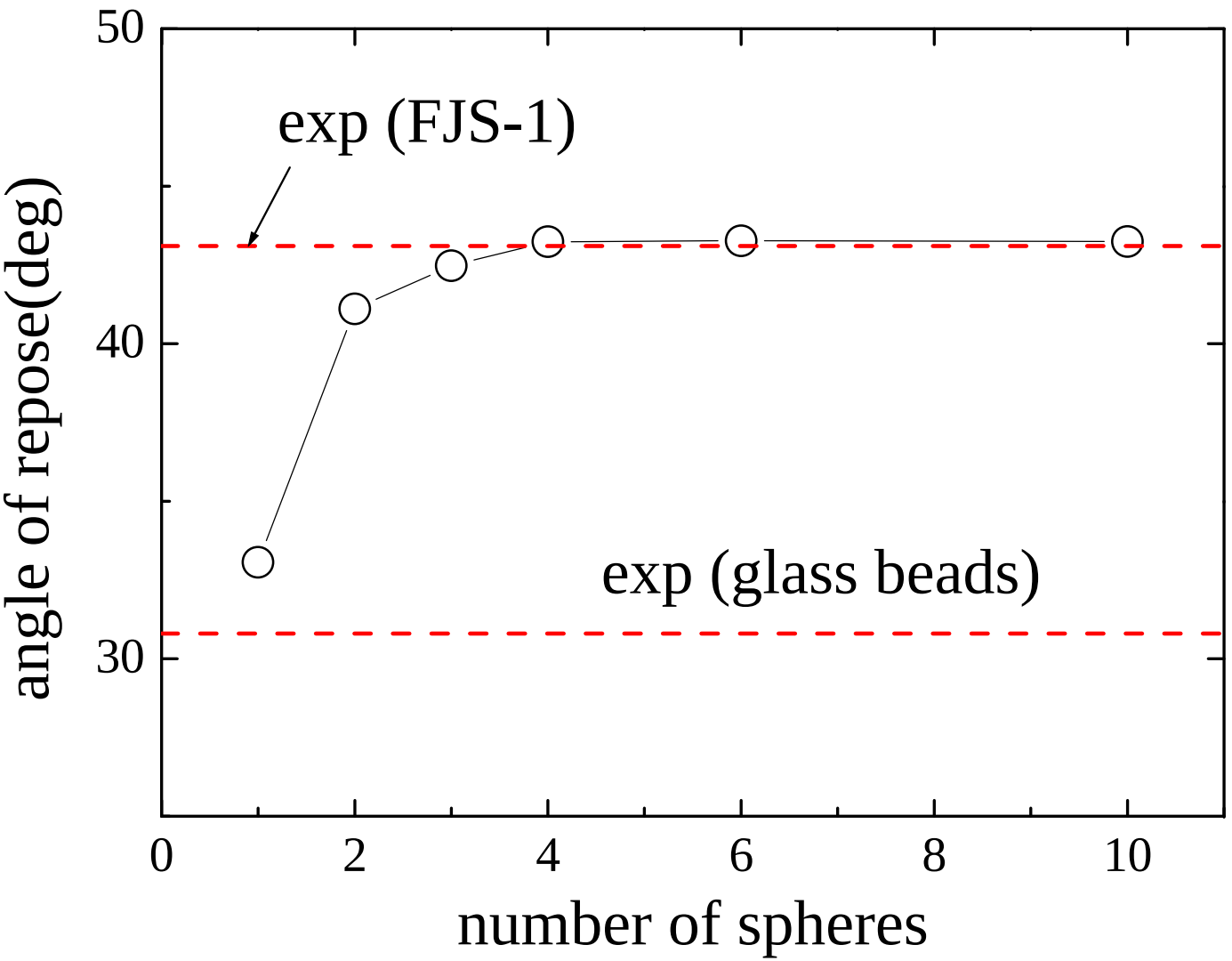

Particle shape effect: The mechanism

Matsushima, P&G2005

Contact force chain

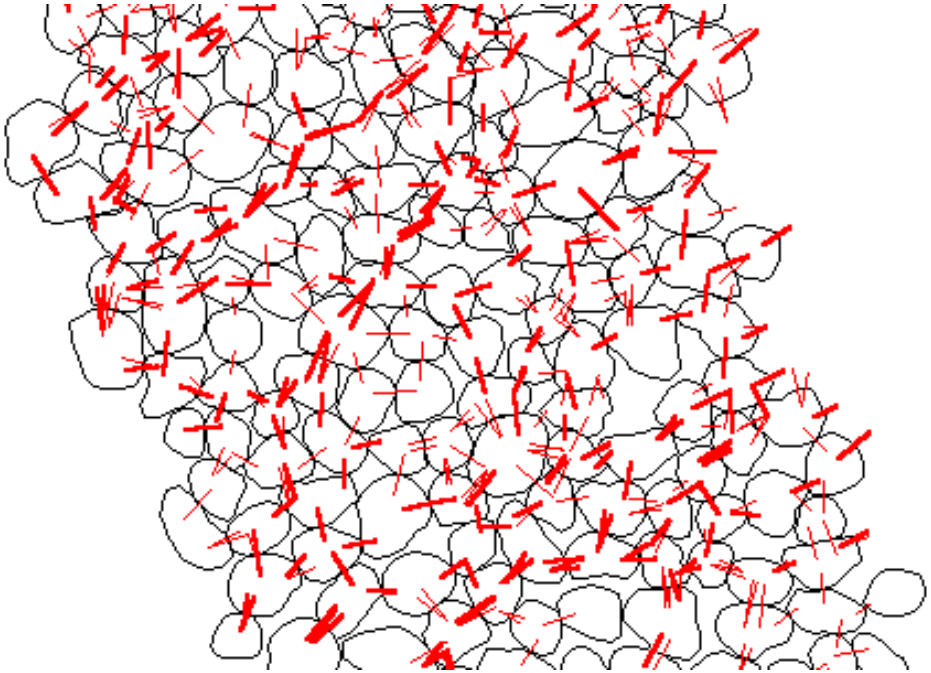

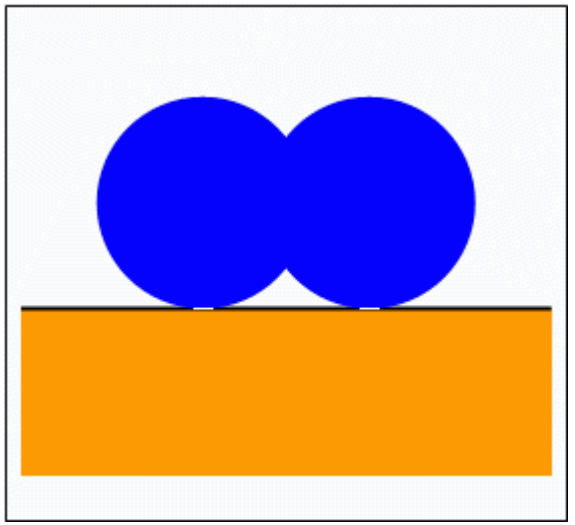

Plural contact points between two grains

→ rolling resistance

→ overall shape is important

Conclusions

Application of Granular Mechanics into geomaterials has been tried for decades.

Some breakthrough has been found recently (in my opinion).

Recent progress of various technologies makes it push forward.

References

Chang, C.-S. and Misra, A. 1990a. Application of uniform strain theory to heterogeneous granular solids, J. Eng. Mech., ASCE, 116, 10, 2310-2329.
Chang, C.-S. and Misra, A. 1990b. Packing structure and me-chanical properties of granulates, J. Eng. Mech., ASCE, 116, 5, 1077-1093.
Smith, W.O., Foote, P.D., Busang, P.F. 1929. Packing of ho-mogeneous spheres, Physical Review, 34, 1271-1274.
Heiken, G.H., Vaniman, D.T., French, B.M. editors (1991). Lunar Sourcebook, Cambridge University Press, 1991.
Matsushima, T. and Chang, C-S. 2006. Proc. IS-Yamaguchi, (submitted).
Matsushima, T. and Saomoto, H. (2002). Discrete element modeling for irregularly-shaped sand grains, Proc. NUMGE2002: Numerical Methods in Geotechnical Engineering, Mestat (ed.), 239-246.
Matsushima, T. (2004). 3-D Image-based Discrete Element Modeling for Irregularly-Shaped Grains, Proc. 2nd International PFC Symposium.

References

Matsushima, T., Saomoto, H., Uesugi, K., Tsuchiyama, A. and Nakano, T. (2004). Detection of 3-D irregular grain shape of Toyoura sand at SPring-8, X-ray CT for geomaterials: Proc. International workshop on X-ray CT for geomaterials (Otani and Obara eds.), Balkema, 121-126.

Chang, C.-S., Matsushima, T., Lee, X.: Heterogeneous Strain and Bonded Granular Structure Change in Triaxial Specimen Studied by Computer Tomography, Journal of Engineering Mechanics, ASCE. Vol. 129, Issue 11, pp.1295-1307, 2003.

Matsushima, T. et al. (2006.3) Image-based modeling of Lunar soil simulant for 3-D DEM simulations, Earth & Space 2006 (CD-ROM). (to be submitted to J. Aerospace Eng., ASCE).

Matsushima, T. (2005) Effect of irregular grain shape on quasi-static shear behavior of granular assembly, Proc. Powders & Grains 2005.